

Neural Mechanisms of Facial Emotion Recognition in Autism: Distinct Roles for Anterior Cingulate and dIPFC

John A. Richey, Denis Gracanin, Stephen LaConte, Jonathan Lisinski, Inyoung Kim, Marika Coffman, Ligia Antezana, Corinne N. Carlton, Katelyn M. Garcia & Susan W. White

To cite this article: John A. Richey, Denis Gracanin, Stephen LaConte, Jonathan Lisinski, Inyoung Kim, Marika Coffman, Ligia Antezana, Corinne N. Carlton, Katelyn M. Garcia & Susan W. White (2022): Neural Mechanisms of Facial Emotion Recognition in Autism: Distinct Roles for Anterior Cingulate and dIPFC, Journal of Clinical Child & Adolescent Psychology, DOI: [10.1080/15374416.2022.2051528](https://doi.org/10.1080/15374416.2022.2051528)

To link to this article: <https://doi.org/10.1080/15374416.2022.2051528>



Published online: 27 Apr 2022.



Submit your article to this journal [↗](#)



Article views: 6



View related articles [↗](#)



View Crossmark data [↗](#)



Neural Mechanisms of Facial Emotion Recognition in Autism: Distinct Roles for Anterior Cingulate and dIPFC

John A. Richey^a, Denis Gracanin^b, Stephen LaConte^{c,d}, Jonathan Lisinski^c, Inyoung Kim^{c,e}, Marika Coffman^{a,f,g}, Ligia Antezana^a, Corinne N. Carlton^a, Katelyn M. Garcia^a, and Susan W. White^h

^aDepartment of Psychology, Virginia Tech; ^bDepartment of Computer Science, Virginia Tech; ^cFralin Biomedical Research Institute at Virginia Tech Carilion; ^dDepartment of Biomedical Engineering and Mechanics, Virginia Tech; ^eDepartment of Statistics, Virginia Tech; ^fCenter for Autism and Brain Development, Duke University; ^gDepartment of Psychiatry and Behavioral Sciences, Duke University; ^hDepartment of Psychology, Center for Youth Development and Intervention, University of Alabama

ABSTRACT

Objective: The present study sought to measure and internally validate neural markers of facial emotion recognition (FER) in adolescents and young adults with ASD to inform targeted intervention.

Method: We utilized fMRI to measure patterns of brain activity among individuals with ASD ($N = 21$) and matched controls (CON; $N = 20$) 2 s prior to judgments about the identity of six distinct facial emotions (happy, sad, angry, surprised, fearful, disgust).

Results: Predictive modeling of fMRI data (support vector classification; SVC) identified mechanistic roles for brain regions that forecasted correct and incorrect identification of facial emotion as well as sources of errors over these decisions. BOLD signal activation in bilateral insula, anterior cingulate (ACC) and right dorsolateral prefrontal cortex (dIPFC) preceded accurate FER in both controls and ASD. Predictive modeling utilizing SVC confirmed the utility of ACC in forecasting correct decisions in controls but not ASD, and further indicated that a region within the right dIPFC was the source of a type 1 error signal in ASD (i.e. neural marker reflecting an impending correct judgment followed by an incorrect behavioral response) approximately two seconds prior to emotion judgments during fMRI.

Conclusions: ACC forecasted correct decisions only among control participants. Right dIPFC was the source of a false-positive signal immediately prior to an error about the nature of a facial emotion in adolescents and young adults with ASD, potentially consistent with prior work indicating that dIPFC may play a role in attention to and regulation of emotional experience.

Substantial prior work indicates that individuals with Autism Spectrum Disorder (ASD) have difficulty in recognizing nonverbal cues communicated through the face (Black et al., 2017; Harms et al., 2010). Such difficulties in facial emotion recognition (FER) may prevent appropriate coordination of subsequent socio-emotional responses among affected individuals, thereby exacerbating the social dysfunction that is the hallmark of ASD. Evidence further suggests that FER deficits are correlated with social disability among individuals with ASD (García-Villamizar et al., 2010) and confer functional impairment above and beyond core symptoms (Wallace et al., 2011). Yet, the broader body of work examining FER deficits among children and adults with ASD contains surprisingly inconsistent results, with some empirical work demonstrating little or no difference in emotion recognition accuracy (Castelli, 2005; Evers et al., 2014; Jones et al., 2011; Lacroix et al., 2009; Spezio et al., 2007),

and others reporting profound differences between clinically diagnosed individuals and typically developing peers (Baron-Cohen et al., 1997; Grossman et al., 2000; Ogai et al., 2003). This lack of clarity represents a systematic barrier to future work, as the absence of consistent, replicable markers indicate the presence and progression of ASD inhibits both the development and also the measurement of FER intervention concepts. Accordingly, the purpose of the work outlined here was to utilize fMRI to identify shared and distinct brain regions that reliably forecast accurate versus inaccurate decisions about the types of facially displayed emotion in adolescents and young adults with ASD versus matched controls. To this end, we used a novel fMRI task in combination with a machine learning approach (support vector classification; SVC), in order to establish a replicable set of neurofunctional markers that are associated with both success and failure in recognizing facial emotions.

CONTACT John A. Richey ✉ richey@vt.edu 📧 Department of Psychology, Virginia Tech, Or by Surface Mail To: John A. Richey, MC0436, 109 Williams Hall, Blacksburg, VA 24061, USA

Although a single consensus definition of FER remains elusive, this complex social-cognitive process has been operationally defined as the ability to accurately detect emotional content expressed nonverbally through specific configurations of facial-muscle movements (Ekman, 1970). Among typically developing children, the ability to recognize and respond to such facially displayed emotion emerges in infancy, and continues to improve across childhood and into adolescence (Barrera & Maurer, 1981; Batty & Taylor, 2006; Lenti et al., 1999). Gleaning emotional content from facial cues is further thought to play a critical role in the development of social competence and interpersonal relationship development by facilitating adjustments in self-behaviors (see Turner & Stets, 2006 for a sociological view) and formulation of appropriate emotional responses during reciprocal social interactions (Hess et al., 2016; Hopkins et al., 2011). For example, it has been hypothesized elsewhere that the real-time construction of appropriate or expected emotional responses to an interaction partner during dynamic social contexts is necessarily predicated upon accurate identification of that partner's nonverbal emotions, principally those displayed through the face (Mier et al., 2010; Shanton & Goldman, 2010). It can be inferred consequently that interpretation of nonverbal facial expressions may be essential to updating privately held internal states and subsequent behavioral responses (Goldman & Sripada, 2005). However, as recently noted in a comprehensive review by Barrett and colleagues (2019), the vast complexity inherent in FER presents a substantial challenge to understanding its neural bases. For example, there appears to be no evidence for a singular or one-to-one mapping between particular facial movements and a specific underlying emotional category, nor is there evidence in the converse for a consistent facial configuration linked to a specific emotional state. This suggests, at minimum, that FER processes and their underlying neurofunctional substrates are not purely axiomatic or deterministic (i.e. a particular combination of facial movements does not perfectly correlate to a unique emotional state), but rather are a dynamic assembly of neurally defined interpretive processes that are integrated into a precept of a partner's hidden mental category.

Studies examining the functional properties of these neural circuits provide some insight into their basic organizational principles as well as how their response properties change over the course of development. Brain imaging studies in humans have identified that face processing occurs in several distributed cortical and subcortical regions, some of which appear to be modulated by both emotion type as well as affective

significance. For example, in response to static facial expressions, activity has been reported in core face-processing regions including fusiform gyri (Johnston et al., 2005; Kawasaki et al., 2012), amygdala (Adolphs, 2002; Herrington et al., 2011), insula (Boucher et al., 2015), superior temporal sulcus (STS; Said et al., 2010) and anterior cingulate cortex (ACC; Fan et al., 2011). Prior work using both positron emission tomography (PET; George et al., 1993; Lane et al., 1997) and fMRI have further suggested that ACC is a key integration area for the conscious experience of emotion (e.g. Gu et al., 2013), perhaps due to its role in merging interoceptive and autonomic activity with high-order cortical functions (Medford & Critchley, 2010; Stevens et al., 2011). These areas also appear to be involved in recognizing emotion from dynamic faces at various points in time, particularly the STS and V5 (Furl et al., 2015). However, dynamic faces also invoke activation in frontal areas including inferior and orbital frontal gyri (Schultz & Pilz, 2009). When manipulated experimentally, distinct elements of facially displayed emotions such as salience, intensity and motivational valence appear to systematically but differentially modulate BOLD signal activity across these regions (Pourtois et al., 2013; Vuilleumier & Pourtois, 2007), suggesting that FER comprises distinct levels of processing with essential feedback interactions across regions. More specifically, interactions among these spatially distributed but highly interconnected brain regions appear to give rise to at least two important mechanisms involved in accurate determinations about the identity of facially displayed emotion: (1) simulation of the observed emotion in the perceiver and (2) the modulation of sensory cortices via top-down influence (Adolphs, 2002; Kveraga et al., 2007; Wood et al., 2016). The first process involves extraction of sensory information, primarily the geometric structural properties of the image, and may further involve amygdala and orbitofrontal cortices to allow fine-tuning of the categorization of facial emotion and enhance allocation of attention to its most relevant features (Leppänen & Nelson, 2009). In parallel with or subsequent to perceptual information extraction, the amygdala and orbitofrontal cortices likely trigger representational memory and associated knowledge via projections to executive regions of the neocortex including the dorsolateral prefrontal cortex (dlPFC; Bar, 2003) and hippocampal formation (Anderson et al., 2016). This latter mechanism appears to be independent of the discrete emotional category (Lindquist et al., 2012) but may contribute uniquely to the retrieval of conceptual knowledge about the emotion via prior experience (Bar, 2007; Wilson-Mendenhall et al., 2011). Thus, the accurate perception of facial emotion is most likely predicated

upon multiple intertwined neural processes that compare the sensory properties of a visually perceived facial emotion against a semipermanent storehouse of exemplars maintained in participating cortical regions.

Patterns of activation in these cortical and subcortical regions have been found in previous studies to be systematically altered among youth and adults with ASD. Indeed, behavioral deficits in FER in ASD samples have been observed behaviorally for some time (e.g. Hobson, 1986a; Macdonald et al., 1989), and as early as Kanner's (1943) original description have been theorized to be mechanistically related to many of the functional deficits observed in the disorder. More recent empirical work has probed the potential neural bases of these deficits using a variety of techniques including electroencephalography (EEG) PET and fMRI (see Harms et al., 2010; Black et al., 2017 for reviews). Most, although not all neuroimaging studies of FER in ASD report reduced or absent limbic and/or visual cortical activation, particularly fusiform gyrus as compared to typically developing peers. For example, Critchley et al. (2000) were among the first to probe this question using fMRI, and found that during a task requiring forced choices about happy and angry faces, reduced BOLD signal activity was observed in the fusiform gyrus during explicit processing of emotional faces, as well as decreased amygdala and cerebellar activity during implicit processing (gender identification) conditions. These effects have been observed in more recent work (Deeley et al., 2007; Scherf et al., 2010; Styliadis et al., 2021), as well as abnormal activity in the superior temporal sulcus (STS; Hadjikhani et al., 2007; Humphreys et al., 2008; Pelphrey et al., 2005) and amygdala (Kliemann et al., 2012), perhaps reflecting a failure of feedback interactions between cortical and limbic structures. fMRI evidence derived from meta-analysis has also revealed that FER in ASD is associated with decreased activation in somatosensory cortices and hypothalamus, as well as increased activation in subcortical activation such as caudate and precuneus (Aoki et al., 2015; Sugranyes et al., 2011). Overall, results appear to support a general hypothesis of dysfunctional cortical–subcortical interactions, particularly centered around limbic modulation of visual cortices.

Despite the general trends reported across meta-analysis, individual studies continue to report disparate results, which have been attributed to a variety of participant and experiment-related factors (Garman et al., 2016; Harms et al., 2010; Nuske et al., 2013; Shanok et al., 2019; Uljarevic & Hamilton, 2013). Consequently, the characterization of replicable

neurobiological markers that could be used to predict and examine the effects of treatment and the degree to which change in those markers relates to a clinical effect remains a largely unmet challenge. In addition, given the substantial complexity inherent in decoding facial emotions, particularly when considering individual types of emotion and their motivational valence (e.g. Feldman-Barrett et al., 2019), the basic neural mechanisms underlying basic correct and incorrect choices about facial emotion identity remain incompletely understood. Accordingly, the purpose of the present investigation was to test the overall hypothesis that predictive statistical techniques, when applied to fMRI data, could identify regions of the brain that temporally predict (approximately two seconds prior to) successes as well as failures in individual emotion recognition decisions among adolescent and young adult men of normal IQ with and without ASD. Overall, we hypothesized that neurobiological markers in regions of the brain that have been previously identified as involved in FER among typically developing controls would be implicated in the commission of errors among individuals with ASD and further that the classification of brain states prior to subjective perception of emotion recognition would contain both overlapping as well as distinctive patterns of evoked responses, the latter of which would distinguish ASD from typically developing peers. Based upon prior work supporting the utility of fMRI for accurate, real-time decoding of psychological states (see LaConte, 2011 for review), we applied a model-based machine-learning approach to a novel FER task in order to (1) decode brain states in control participants and those with ASD in the moments leading up to a decision about a facial emotion identity and then (2) predict future decisions about the identity of facial emotions based solely on these patterns of activation.

Methods

Participants

Typically Developing (TD) Comparison Group

The sample of TD adults included 20 men ages 16–30 years.¹ Total sample demographics are presented in Table 1. Participants (both TD and ASD, as below) were recruited through flyers in the local community (e.g. churches, schools, restaurants), existing research registry databases, university-affiliated assessment clinics, and local ASD support groups. In order to be eligible for the study, participants were required to be (1) male;

¹We opted to include only men in this study, based on the following factors: (1) prior work indicating that ASD is predominantly diagnosed in men, (2) evidence that FER abilities may vary by sex, and (3) due to the small sample size sought here.

Table 1. Participant demographics and symptom profiles.

	CON (N = 20)	ASD (N = 21)	t (p)
Age (years)	23.4 (2.87)	21.62 (3.64)	0.23 (.9)
ADOS			
COMM	–	6.1 (4.7)	–
SI	–	8.8 (2.3)	–
SBRI	–	2.3 (1.8)	–
WASI			
Full Scale	110.1 (9.04)	107.04 (15.76)	0.51 (.79)
Verbal	113.3 (14.19)	106.95 (15.31)	0.31 (.91)
Performance	110.03 (12.31)	108.13 (17.59)	0.57 (.88)
SRS			
Aware	6.35 (18.4)	10 (3.11)	3.01 (.005)
Cog	7.3 (4.14)	14.25 (5.13)	3.8 (<.001)
Comm	11.15 (5.24)	26.88 (10.75)	3.9 (<.001)
Mot	8.3 (3.96)	14.81 (4.15)	3.0 (.005)
RRB	6.2 (3.72)	16.81 (8.42)	4.5 (<.001)
Total	39.4 (14.43)	84.1 (18.74)	4.06 (<.001)

Note: WASI = Wechsler Abbreviated Scale of Intelligence, ADOS = Autism Diagnostic Observation Scale, SRS = Social Responsiveness Scale, Aware = awareness, Cog = cognition, Comm = communication, Mot = motivation, RRB = restricted, repetitive behaviors.

(2) between the ages of 16–30 years; (3) of at least average cognitive ability (FSIQ-2 ≥ 80), as confirmed by Wechsler Abbreviated Scale of Intelligence, second edition (WASI-II; Wechsler, 2011); (4) capable of undergoing magnetic resonance imaging (MRI; no contraindications such as metal in body); (5) ambulatory with no known, uncorrected sensory deficits; (6) psychologically healthy (free from severe psychopathology that warrants immediate treatment, as confirmed by a clinical interview (Anxiety Disorders Interview Schedule for DSM-5 [ADIS-5, Brown & Barlow, 2014]); (7) have no known genetic, medical, or neurological condition including intellectual disability; and (8) not in treatment that directly targets facial emotion recognition. Twelve individuals (60%) from the TD group self-identified as White/Caucasian, three (15%) identified as Black/African-American, four (20%) identified as Asian, and one individual (5%) self-identified as Middle Eastern descent.

ASD Sample

The sample of adults with ASD included 23 men ages 16–30 years recruited according to the methods as described earlier. Inclusion criteria for the ASD group required a (1) diagnosis of Autism Spectrum Disorder as confirmed by Autism Diagnostic Observation Schedule, Second Edition (ADOS-2; Lord et al., 2012); (2) no changes in medication for 4 weeks, (3) no planned changes in immediate future; and (4) no use of anti-seizure medication. Sixteen individuals (69.5%) self-identified as White/Caucasian, three (13.04%) self-identified as Asian, one (4.34%) identified as Native American, and two (8.6%) self-identified as mixed-

race. Demographic information was unavailable for one individual from the ASD group. Both groups completed the Social Responsiveness Scale (SRS; Constantino et al., 2003), a continuous measure of ASD symptom severity.

Procedure

Interested participants completed an initial phone screen to answer preliminary eligibility questions including a brief MRI safety screener, followed by one in-lab session to confirm study eligibility. All procedures described here were reviewed and approved by the local Institutional Review Board (IRB). Before collecting any data, all adult participants signed a consent form, while adolescents in this study signed an assent form and their parents signed a parent permission form for their child to participate in the study. If they met all inclusion criteria, participants were then scheduled for a pre-treatment assessment, where they completed several questionnaires and behavioral tasks. The pre-treatment assessment visit lasted approximately 3 hours in length and included an Emotion Recognition Task (described below) that was administered during an fMRI scan. The remaining tasks and questionnaires were completed outside of the scanner in a private testing room. All participants received \$20 for the screen session, \$20 for the pre-treatment assessment session, and \$25 for the fMRI scan in addition to compensation for the treatment sessions, posttreatment assessment and follow-up assessment for which data are not reported in this study.

fMRI Paradigm: The Emotion Recognition Task (ERT)

Stimuli. Stimuli for the Emotion Recognition Task (ERT) were drawn from the standardized Cohn-Kanade extended (CK+) action unit (AU)-coded facial expression database (Cohn et al., 1999; Kanade, Cohn & Tian, 2000; Lucey et al., 2010). The CK+ database contains approximately 500 dynamic image sequences ('videos') from 100 actors, and meta-data for each image sequence include annotation of the Facial Action Coding System (FACS; Ekman & Friesen, 1978) AUs, as well as validation data on inter-rater reliability and validity for emotion-labeled expressions. Actors used here ranged in age from 18 to 30 years. Sixty-five percent of actors were women, although because we recruited only male participants in our study we used only male actors from the CK+ image database. Fifteen percent were African-American, 3% were Asian or Latinx, and the remaining were White/Caucasian. Each dynamic, morphing image sequence in the CK+ database begins from a neutral or nearly neutral face (0% emotion intensity), and continually morphs into

a maximally displayed emotion or ‘apex’ (100% emotion intensity). Image sequences used in the current study were continuously morphing (i.e. dynamic) frontal views progressing from 0% until apex, presented in 640×480 8-bit grayscale. As originally reported in Kanade, Cohn and Tian (2000), actors were instructed to perform 23 different facial displays, comprising combinations of AUs. Here, we focused on so-called basic emotions that can be most reliably recognized from facial expressions: happy, sad, surprise, fear, anger, disgust and sadness (Ekman, 1970). We furthermore used only image sequences for these basic expressions that had previously achieved 80% or greater inter-rater agreement on facial emotion identity at apex, based on the available validation metadata. Given the relatively slow temporal resolution of fMRI in capturing hemodynamic responses of interest, we opted to present dynamic sequences in relatively slow-motion, at approximately 25% of “real-time.” On average, the videos were 20.57 seconds ($SD = 7.26$) in length across different emotions and did not vary in length across emotional conditions.

To select the final dynamic image set for use here, two graduate research assistants reviewed and consensus rated the candidate image sequences (i.e. selected from among the six basic emotions and sequences with the highest available inter-rater reliability). From among the eligible sequences, we selected 10 stimuli for each of the six basic emotions for a total of 60 stimuli. The final 60 videos were then split into two sets for two separate functional runs, which therefore included 30 emotion videos or trials per run, and with each emotion shown 5 times per run. In order to mitigate any potential influence of familiarity effects, we limited the number of times that an individual actor was portrayed within a run to three presentations, and no actors were repeated between runs (i.e. any given actor from the CK+ image set appeared in one and only one fMRI run). No videos were repeated at any point within the ERT. The presentation of stimuli within a run was fully randomized for each individual participant to eliminate the possibility of ordering effects.

fMRI Task Procedure. Each participant completed two functional runs of the novel ERT, developed for the purposes of this study. Task conditions and trial timings are summarized in Figure 1. Prior to scanning, all

participants completed a one-on-one training session including a practice task comprising four trials to ensure understanding of task instructions. To further reinforce task instructions, each run began with an instructional screen reiterating task procedures: “Please press the button as soon as you recognize the emotion.” No other instructions were given, nor did we implicitly or explicitly indicate that task performance was tied to any specific incentive, monetary or otherwise.² During the task itself, participants indicated accordingly (via single button press) the earliest moment they recognize the morphing emotion. After recognition was indicated via button press, the video immediately terminated (progressing no further in emotion intensity)³ and a gray fixation cross appeared for approximately 3000 ms. Subsequent to disappearance of the fixation cross, a forced-choice task was presented in which the participant was required to indicate the perceived emotion from the video that had concluded approximately 3000 ms prior. This forced-choice task was presented as plain text and required the participant to highlight a radio-button/checkbox (again via button press) corresponding to one of six basic emotions (happy, sad, angry, fear, disgust, surprise), with the text options always presented in the same order. The forced-choice task was presented with unlimited time, and when the participant selected the emotion, a fixation cross appeared for approximately 3000 ms to conclude the trial. Subsequent to the disappearance of this fixation cross, the next trial started according to the same procedures. No feedback was provided as to whether the previous selection was correct or incorrect. Also, participants were not given the option to skip the forced-choice selection screen nor were they given a ‘don’t know/uncertain’ option. Run 2 was identical to run 1 in all of these respects, but was later used for support vector classification/model validation as described below.

fMRI Data Acquisition

Neuroimaging data were collected using a 3.0 T Siemens Magnetom Trio. Head movement in the scanner was minimized through the use of foam cushions. High-resolution T1-weighted images were acquired using a rapid gradient echo sequence (TR/TE: 2180 ms/

²We further probed the possibility that certain individuals may have been differentially motivated to respond faster to each event because of the implicit relationship between faster responses and the total duration of the run. In other words, it is conceivable that some individuals may have been motivated to respond faster specifically because briefer trials would collectively result in a briefer overall experimental session for that participant. However, we found no correlations between trial number and reaction time or error rate at the group level nor did we observe outliers when evaluating cases individually. We further found no evidence that any participant’s performance approached chance levels in the forced choice phase of the task, thus supporting the notion that participants in general complied with the instructions as given.

³The decision to conclude the morph and transition to a fixation cross was made to avoid the possibility that continuing the morphing sequence could contradict prior belief in the facial emotion identity and therefore introduce noise from other potential psychological processes such as error monitoring and subsequent learning effects. This would have been disproportionately detrimental to isolating BOLD variance on error trials more so than correct trials, and so we designed that task so that a button press would immediately terminate the stimulus and initiate a blank screen with a fixation cross.

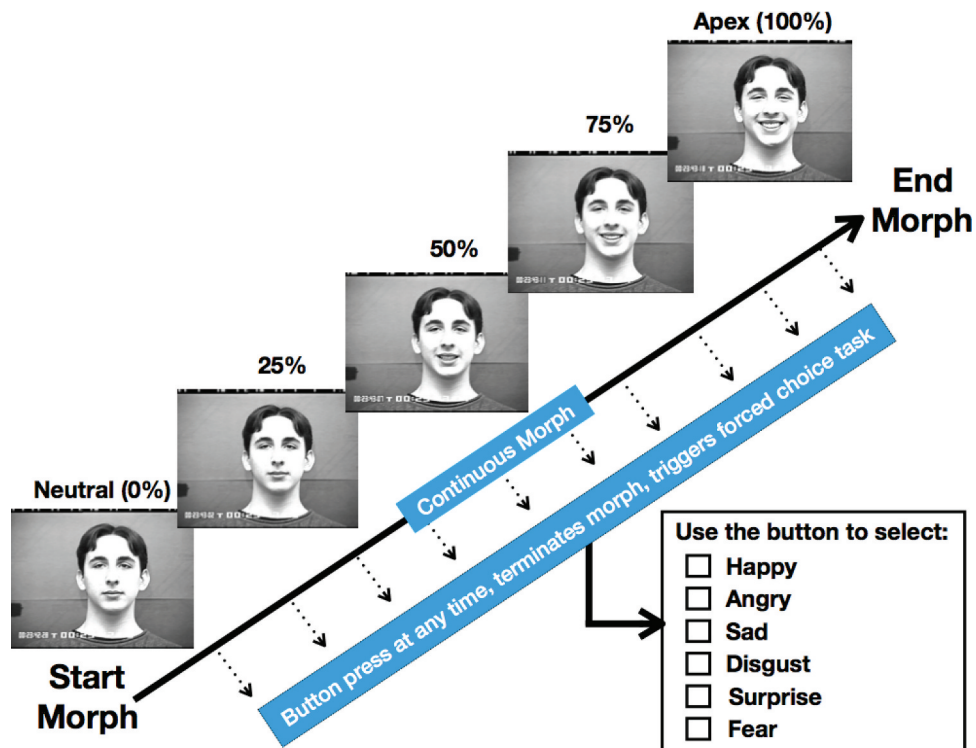


Figure 1. Schematic depiction of Emotion Recognition Task.

3.02 ms; FOV: 22 cm; Image matrix: $184 \times 256 \times 192$; voxel size = $.82 \text{ mm} \times 1.00 \text{ mm} \times 1.00 \text{ mm}$). Functional imaging used an EPI sequence with a repetition time (TR) of 2180 ms, echo time (TE) = 25 ms, flip angle = 90° , 220 mm field of view (FOV), 64×64 matrix. Functional slices were oriented 30° superior-caudal to the plane through the anterior and posterior commissures in order to reduce signal drop-out due to magnetic field inhomogeneities (Deichmann et al., 2003). Each functional image was acquired in an interleaved format, comprising 37.4 mm axial slices for measurement of the BOLD effect, yielding $3.4 \text{ mm} \times 3.4 \text{ mm} \times 4.0 \text{ mm}$ voxels. Runs began with five discarded RF excitations to allow for steady state equilibrium. Data quality was examined using BXH-XCEDE tools (Gadde et al., 2012), an extensible framework for summarizing meta-parameters related to fMRI quality assurance (QA), including but not limited to signal fluctuation-to-noise ratio (SFNR; Greve et al., 2011) and motion/intensity outliers. Results of QA analysis revealed excellent fMRI system stability and data quality with no evidence for systemic artifacts. As such, no participant was discarded due to issues related to data quality.

fMRI Preprocessing and Analytic Approach

Separation of brain tissue from the skull was accomplished using the brain extraction tool (Smith, 2002) in FSL version 4.1.4 (Oxford Center for Functional

Magnetic Resonance Imaging of the Brain, Oxford University, UK). Preprocessing of functional data was accomplished in Statistical Parametric Mapping software (SPM12; Wellcome Department of Cognitive Neurology; <http://www.fil.ion.ucl.ac.uk/spm>) as implemented in Nipype (Gorgolewski et al., 2011), a Python-based framework designed for highly pipelined processing of fMRI data from several neuroimaging packages (<http://nipype.org/nipype>). Our Nipype code is available for evaluation and download at <https://github.com/scanlab-admin/FER>. Preprocessing of fMRI data was conducted in the following steps: (1) slice timing correction temporally aligned the interleaved functional images; (2) correction to the middle functional image was then performed using a six-parameter rigid-body transformation; and (3) functional images were co-registered to structural images in native space. For this co-registration step, functional-to-structural 6 DOF (rigid body) transformations were carried out using brain-boundary-based registration (*bbregister*; Greve & Fischl, 2009) which uses the geometry information of the gray-white matter boundary derived from the automated cortical/subcortical parcellation stream in Freesurfer v7 (<http://surfer.nmr.mgh.harvard.edu/>; Fischl et al., 2004; Fischl et al., 2004) to conduct cross-modal registration within-participants. Next, structural images were normalized into a standard stereotaxic space (Montreal Neurological Institute) for intersubject

comparison using a diffeomorphic warp as implemented in the Advanced Normalization Tools (ANTS; Avants et al., 2011). The same transformation matrices used for structural-to-standard transformations were then used for functional-to-standard space transformations of co-registered functional images. Data were spatially smoothed using a 5-mm isotropic (Gaussian) kernel and then high-pass filtered (128s width) in the temporal domain. Subsequent statistical analyses focused on changes in blood oxygen level dependent (BOLD) contrast (henceforth ‘activation’). To assess motion and related artifacts, we used the ‘RapidArt’ module in NiPype, which detects outlier volumes in a functional imaging data series. Intensity and motion data parameters assessed by RapidArt were then used at the contrast estimation stage to deweight the influence of outlier volumes based on volume-wise motion (>0.5 mm) and/or intensity (± 3 SD) confounds.

fMRI Event Definition. Individual fMRI events of interest were landmarked by a button press from the participant to indicate emotion recognition. That is, as the dynamic image advanced in intensity from neutral (0%) to apex (100%) participants were instructed to press the button at any point during this progression when they believed they knew the displayed emotion (i.e. happy, sad, angry, fear, disgust, surprise), at which point the task immediately advanced to a fixation cross and then forced-choice screen (white text on black background). Two thousand milliseconds were subtracted from this temporal landmark (defined by the button press) in order to access the functional volume that *immediately preceded* the report of subjective recognition. We defined events in this manner in order to index neurofunctional processes involved in the construction of (but not the aftermath of reporting) a single precept for perceived facial emotion. All such defined events were constrained to a total duration of 2000 ms in SPM12, and thus spanned precisely 2 s up to but not including neural activation during or subsequent to the button press. Based on these user-defined landmarks in the functional run, we estimated the fixed-effects general linear model (GLM) for BOLD responses with an autoregressive (AR[1]) structure in SPM12. The AR model corrects for temporal autocorrelation of the residuals in fMRI data, thus reducing the potential for false positives in the Restricted Maximum Likelihood (ReML) parameter estimation approach. For all first level effects, “correct” trials were those in which the participant selected the textual descriptor (e.g., happy, angry, sad, disgust, fear or surprise) in the forced-choice

phase of the task (Figure 1), which matched the prior AU-coded validation data for that face (i.e. angry face judged as angry). “Incorrect trials were those in which the participant selected any other identifier (i.e. angry face judged as anything other than angry). Regressors for “correct” and “incorrect” trials were convolved with a double-y function and its first temporal derivative to model the hemodynamic response of the entire duration of each event. Six movement parameters of the (rigid body) realignment were included in the design matrix as additional regressors.

General Linear Model. Group-wise activation and deactivation images were calculated by a mixed effects (mixed model ANOVA) higher level analysis using a whole-brain univariate GLM in which we regressed the preprocessed and spatially smoothed BOLD signal on the 2000 ms period immediately preceding the button press. We also included the time series of six head motion parameters as regressors of no interest and deweighted outlier volumes based on motion (>0.5 mm displacement) and intensity (± 3 SD). The following models were evaluated for correct and incorrect judgments as well as correct $>$ incorrect: (1) CON (mean), (2) ASD (mean), (3) CON $>$ ASD, (4) CON+ASD. All results were initially thresholded at $Z > 2.0$ (two-tailed) and were false discovery rate (FDR) corrected at $p < .05$. Effects surviving this initial lenient threshold were subsequently corrected at $Z > 3.3$ to aid interpretability.

Support Vector Classification (SVC) via Fast Regularized Ensemble of Models (Frem)

Support Vector Classification (SVC) is a machine learning (ML) approach for data classification, and is frequently used to make forward predictions about a condition of interest based on stored patterns of brain activation (Haxby et al., 2001; LaConte et al., 2005). Linear support vector machines have shown good performance in small sample situations such as ours (Matykievicz & Pestian, 2012), but come with a high computational cost (Hoyos-Idrobo et al., 2018) and are susceptible to bias as they involve fitting models on a fraction of the data which can introduce instability when the number of features is small, as is the case here. We therefore opted to use a model aggregation or ensembling method, which averages the output of several suitable models to reduce the variability of the output of the decoder and balance the two opposing effects of model stability and bias.⁴ Specifically, we utilized an

⁴Stability is defined as the amount of change in the output of the decoder as a function of small changes in the data on which the decoder is trained (Shalev-Shwartz et al., 2010).

ROI-based forward prediction strategy to train regularized ensembles of models (Fast Regularized Ensemble of Models; FReM; Hoyos-Idrobo et al., 2018), which has shown good performance in small-sample recovery of stable decoders. The FReM approach utilizes a training set to construct a nested cross-validation loop, and inside each fold the best performing (i.e. greatest predictive power) estimator is selected. A forward estimator is then built by averaging all stored models from cross-validation, similar in principle to bootstrap aggregating (bagging; Breiman, 1996), but with improved stability in weight maps (Hoyos-Idrobo et al., 2018). Prediction over conditions (application of training to test data) can be summarized in terms of accuracy rates in forecasting experimental condition in never-seen data (0.0–1.0) as well as type I and II error rates, which can then be compared against random prediction to ascertain the overall performance of the estimator. “Random” chance in this case was assumed to be 0.5, which was further confirmed by a random prediction model that was identical to the primary model in every respect (identical tuning parameters), but ignoring the input features. This dummy model concurrently established the performance of the estimator without priors, thus serving as a baseline for comparing the actual SVC model to random guesses, which in each case were confirmed to yield accuracy rates of 0.5. All FReM models reported here were implemented in NiLearn 8.0 (itself based on Scikit-learn; Abraham et al., 2014), a Python-based framework for statistical and machine learning tools for fMRI data. The NiLearn code used to produce all results reported here is available for download and review at <https://github.com/scanlab-admin/FER>.

In the current study, we trained a 10-fold cross-validated estimator on run 1 utilizing voxels within individual significant clusters defined by event-related fMRI analysis. We specifically examined clusters from our event-related analysis of run 1 which forecasted a correct and incorrect decision 2000 ms prior to a button press. These events were segregated into trials that resulted in either a (1) correct or (2) incorrect decision about a facial emotion identity to create a model of neural activation corresponding to correct and incorrect decisions. To forward predict behavioral outcomes (i.e. predict correct and incorrect choices about a facial emotion) based on patterns of brain activation observed in run 1, we collected a second functional run, identical in structure to the first, although with new actors and dynamic images. The basic premise motivating this approach was to answer the question: is it possible to utilize neural data to outperform chance in predicting a correct and/or incorrect decision about facial emotion identity in “never seen” data in run 2 (test data)?

Results

Cognitive Functioning and Self-Reported Symptoms

Results for self-reported symptoms and IQ measurements are reported in Table 1.

Emotion Recognition Task – Behavioral Performance

Accuracy in rates of FER were not statistically different across groups when evaluating task performance as a whole as well as when evaluating individual emotions (all $p \geq .34$), nor was task performance related to chronological age in either group. The ASD group required approximately 23.34% additional time, per trial, for a given dynamic image in order to make a correct choice, a finding that did not reach statistical significance, and we further found that the eventual correctness of a decision did not relate to the amount of time elapsed for any emotion type (all $ps \geq .29$). Thus, behavioral performance of the ERT did not distinguish between groups.

fMRI Statistical Comparisons

For run 1, a whole-brain mixed-model ANOVA compared voxel-wise activity for controls and ASD for each response category (correct [COR] and incorrect [INC] emotion recognition trials) for the 2000 ms that immediately preceded the button press indicating the participant believed he/she recognized the displayed emotion. Main effect images and corresponding activation tables are provided in Figures 2 and 3, and Tables 2 through 5, respectively. To first examine distinct, or nonshared effects associated with correct and incorrect decisions, we examined effects observed for the contrast CON>ASD within the mixed-model ANOVA. In this between-groups contrast, a significant main effect was observed only for COR trials, in a single large cluster ($k = 15,845$, peak voxel MNI[x,y,z]: $-61, 12, 11$, $t = 4.12$) covering both cortical and subcortical regions. This suggests that these regions were utilized by controls and not ASD prior to a correct decision. However, no significant clusters were observed at a similar threshold for the main effect of INC, nor for the contrast of COR>INC (Table 4; Figure 2). We then probed for effects that were unique to ASD by evaluating the inverse groupwise contrast (i.e. for ASD>CON), and found that no significant clusters were observed for either main effects (CON, INC) or interaction (COR>INC). Collectively, these results suggested that there were a number of brain regions covered by a single cluster that were

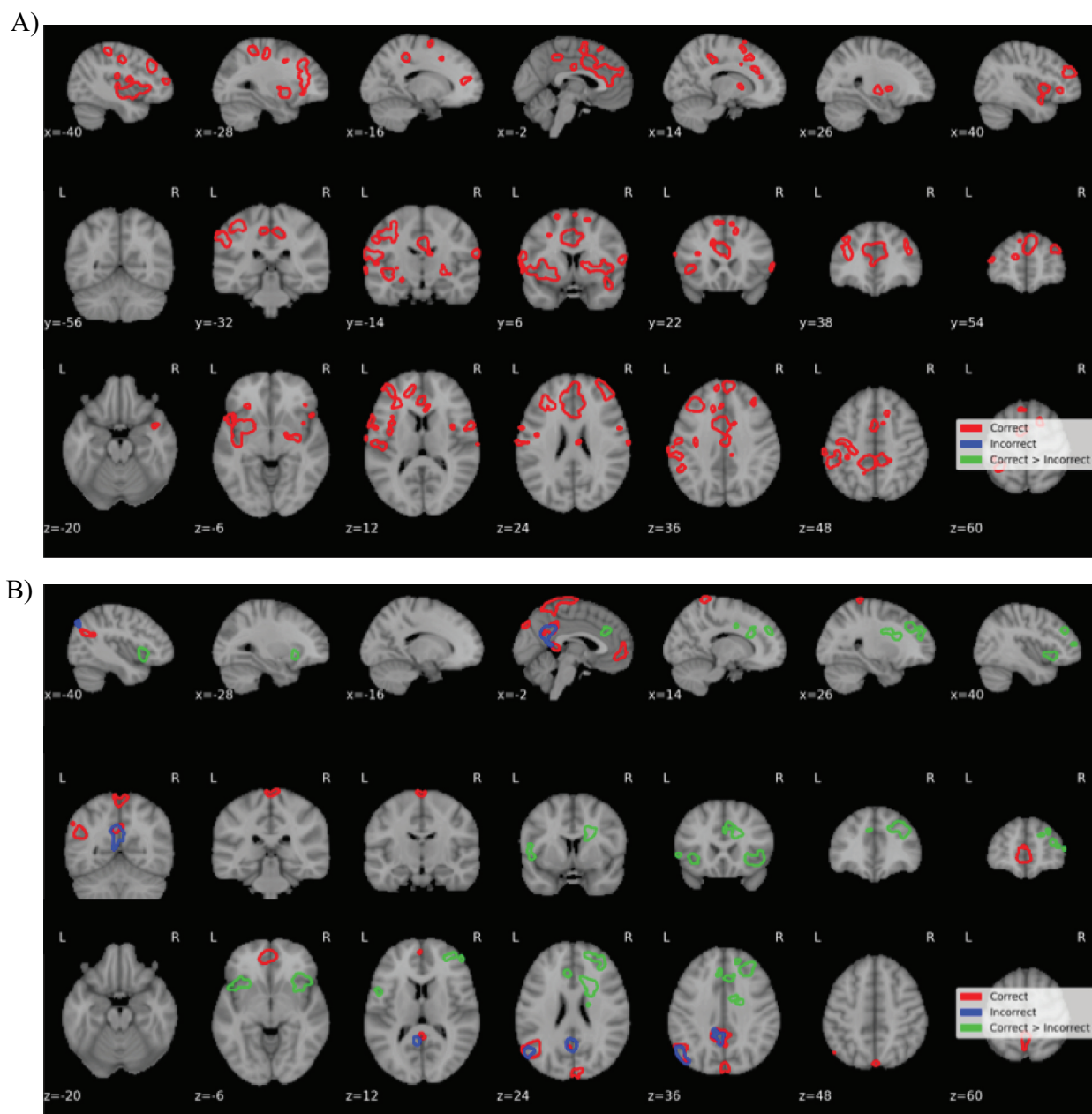


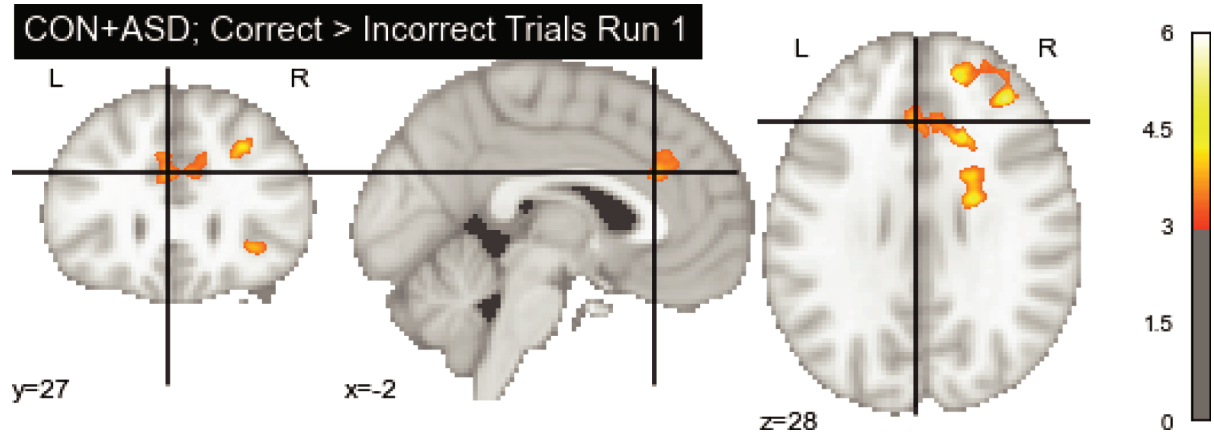
Figure 2. (A) Mixed effects ANOVA (CON>ASD) indicates main effect of group for COR, but not INC or their interaction 2 s prior to button press. All p s <.05; FDR corrected. (B) Combined sample (CON+ASD) indicates significant within-participants effects associated with correct and incorrect decisions as well as COR>INC, 2 s prior to button press. All p s <.001; FDR corrected.

utilized by controls but not ASD to arrive at a correct decision, although rates of accuracy were not statistically different between groups.

To evaluate shared mechanisms of emotion recognition, or in other words to identify effects that were observed in the total sample (i.e. for the groupwise effect of CON+ASD), we evaluated the main effects (COR, INC) and interaction (COR>INC) terms using a similar whole-brain approach for each within-participants contrast. Results of this analysis revealed a relatively constrained set of activation patterns in six clusters for COR, including left middle temporal gyrus

($k = 669$, peak voxel MNI[x,y,z]: $-51, -65, 27, t = 5.56$) and left precuneus ($k = 357$, peak voxel MNI[x,y,z]: $-6, -47, 31, t = 4.45$; see Table 5 for descriptors of remaining clusters). Incorrect decisions in the combined analysis were associated only with activation in the left posterior cingulate ($k = 460$, peak voxel MNI[x,y,z]: $-7, -50, 7, t = 4.66$), and left angular gyrus, located in the posterior part of the inferior parietal lobule ($k = 389$, peak voxel MNI[x,y,z]: $-55, -67, 31, t = 5.15$). Replicating prior work (e.g. Ashwin et al., 2007; Domes et al., 2014; Herrington et al., 2015), the within-participants effect for COR>INC revealed

A)



B)

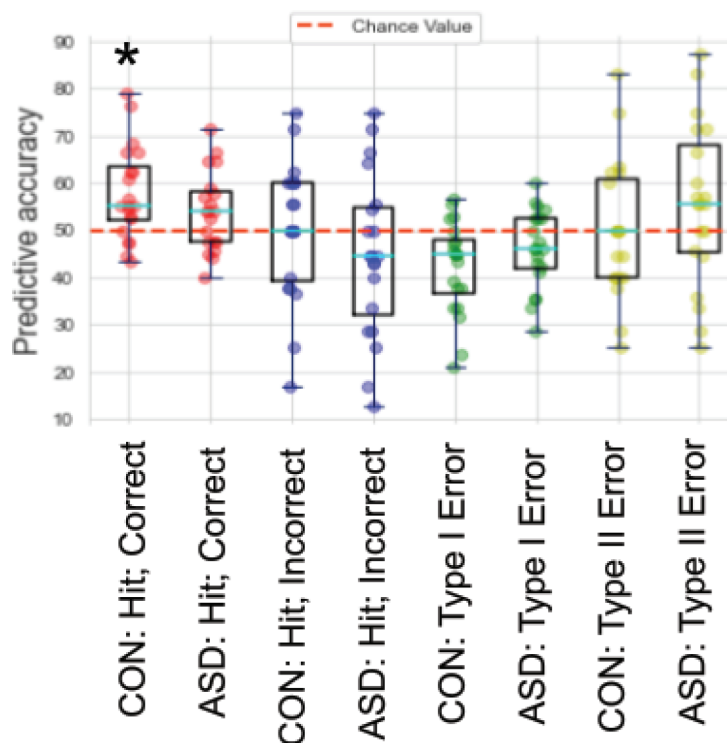


Figure 3. (A) Run 1: ACC cluster (CON+ASD, [CON>INC]; all p s<.001; FDR corrected) utilized for ROI-based SVC prediction. Note this cluster is also displayed in Figure 2, (panel B, green outline). Further note that the ACC cluster targeted by the crosshair is contiguous with the slightly posterior cluster in the transverse plane (rightmost panel), and this single contiguous ACC-focused cluster was used to generate the SVC predictive analysis below in panel B. (B) ROI-based prediction of behavior in run 2 using Support Vector Classification. Relative ACC activation predicts correct decisions among controls beyond chance, but not ASD. Asterisk denotes significant difference from chance (95% CI).

a highly constrained set of results indicating activation in four clusters: anterior cingulate ($k = 700$, peak voxel MNI[x,y,z]: 18, 22, 27, $t = 4.62$), bilateral insula (left $k = 497$, peak voxel MNI[x,y,z]: -43, 15, -2, $t = 4.59$; right $k = 445$, peak voxel MNI[x,y,z]: 37, 21, -5, $t = 4.47$) and right dlPFC, specifically right middle frontal gyrus ($k = 749$, peak voxel MNI[x,y,z]: 37, 37, 29, $t = 5.23$). We also examined the relative presence of

motion and intensity artifacts in each group, to assess whether the observed effects of interest may be related to differential effects of motion (Table 6). Results indicated no differences between groups in either the rate or amplitude of motion or intensity artifacts, suggesting that between-groups effects in our event-related analysis were unlikely to be related to motion confounds.

Table 2. Control participants.

Correct; clusters significant at $p < .01$; FDR corrected at $p < .05$.						
Talairach-Tournoux Atlas Label	Brodmann Area	Size (mm ³)	tMax	MNI Coordinates (Peak)		
				X	Y	Z
Right Cuneus	18	7547	6.15	3	-93	21
Left Medial Frontal Gyrus	10	5513	5.03	-12	50	14
Left Angular Gyrus	39	2207	5.57	-56	-68	34
Left Superior Temporal Gyrus	22	1589	4.54	-68	-17	1
Incorrect; clusters significant at $p < .01$; FDR corrected at $p < .05$.						
Talairach-Tournoux Atlas Label	Brodmann Area	Size (mm ³)	tMax	MNI Coordinates (Peak)		
				X	Y	Z
Left Medial Frontal Gyrus	11	1352	3.95	0	56	-12
Correct>Incorrect; clusters significant at $p < .01$; FDR corrected at $p < .05$.						
Talairach-Tournoux Atlas Label	Brodmann Area	Size (mm ³)	tMax	MNI Coordinates (Peak)		
				X	Y	Z
Right Middle Frontal Gyrus	9	16,961	6.2	37	37	29
Right Cerebellar Tonsil	-	2644	4.96	54	-64	-36

Table 3. ASD participants.

Correct						
Talairach-Tournoux Atlas Label	Brodmann Area	Size (mm ³)	tMax	MNI Coordinates (Peak)		
				X	Y	Z
No Clusters Significant						
Incorrect						
Talairach-Tournoux Atlas Label	Brodmann Area	Size (mm ³)	tMax	MNI Coordinates (Peak)		
				X	Y	Z
No Clusters Significant						
Correct>Incorrect; Clusters significant at $p < .01$; FDR corrected at $p < .05$.						
Talairach-Tournoux Atlas Label	Brodmann Area	Size (mm ³)	tMax	MNI Coordinates (Peak)		
				X	Y	Z
Left Mammillary Body	-	11,122	4.48	-2	-11	-17
Left Inferior Frontal Gyrus	10	3429	3.69	-55	38	0

Table 4. Controls > ASD.

Correct; clusters significant at $p < .05$; FDR corrected at $p < .05$.						
Talairach-Tournoux Atlas Label	Brodmann Area	Size (mm ³)	tMax	MNI Coordinates (Peak)		
				X	Y	Z
Left Inferior Frontal Gyrus	44	15,845	4.12	-61	12	11
Incorrect						
Talairach-Tournoux Atlas Label	Brodmann Area	Size (mm ³)	tMax	MNI Coordinates (Peak)		
				X	Y	Z
No Clusters Significant						
Correct>Incorrect						
Talairach-Tournoux Atlas Label	Brodmann Area	Size (mm ³)	tMax	MNI Coordinates (Peak)		
				X	Y	Z
No Clusters Significant						

Table 5. Control + ASD.

Correct; clusters significant at $p < .001$; FDR corrected at $p < .05$.						
Talairach-Tournoux Atlas Label	Brodmann Area	Size (mm ³)	tMax	MNI Coordinates (Peak)		
				X	Y	Z
No Label	–	882	6.29	5	–36	77
Left Mid-Temporal Gyrus	39	669	5.56	–51	–65	27
Left Precuneus	31	357	4.45	–6	–47	31
Left Medial Frontal Gyrus	10	330	4.47	–7	51	–4
Right Cuneus	19	232	6.15	3	–83	36
Right Posterior Cingulate	29	188	4.42	3	–45	6
Incorrect; clusters significant at $p < .001$; FDR corrected at $p < .05$.						
Talairach-Tournoux Atlas Label	Brodmann Area	Size (mm ³)	tMax	MNI Coordinates (Peak)		
				X	Y	Z
Left Posterior Cingulate		460	4.66	–7	–50	7
	29					
Left Angular Gyrus		389	5.15	–55	–67	31
	39					
Correct>Incorrect; clusters significant at $p < .001$; FDR corrected at $p < .05$.						
Talairach-Tournoux Atlas Label	Brodmann Area	Size (mm ³)	tMax	MNI Coordinates (Peak)		
				X	Y	Z
Right Middle Frontal Gyrus		749	5.23	37	37	29
	9					
Right Anterior Cingulate		700	4.62	18	22	27
	32					
Left Insula		497	4.59	–43	15	–2
	47					
Right Insula		445	4.47	37	21	–5
	47					

Table 6. Characterization of motion and intensity-related artifacts in CON and ASD groups.

	CON	ASD	p Value
Mean displacement, center of mass [x,y,z]	$M = 1.8$ mm SD = 0.2 mm	$M = 2.01$ mm SD = 0.28 mm	.86
% Volumes with mean volume difference >2%	$M = 1.19$ SD = 0.12	$M = 1.37$ SD = 0.18	.83
% Volumes with mean intensity absolute Z-score >3	$M = 1.31$ SD = 0.08	$M = 0.90$ SD = 0.09	.89
% Volumes de-weighted due to motion artifact (>0.5 mm).	$M = 1.22$ SD = 0.43	$M = 1.63$ SD = 0.67	.74
% Volumes de-weighted due to intensity artifact ($\pm 3SD$).	$M = 0.83$ SD = 0.21	$M = 1.01$ SD = 0.4	.91

Note: Mean displacement [x,y,z] reflects global head motion during the imaging session, aggregating both slow drift and sudden movement. Percent volumes with mean differences >2% tracks sudden spikes in motion by calculating the mean intensity of any given volume [minus] mean functional series volume, thus reflecting volume-to-volume drift. Percent volumes with mean intensity absolute Z-score tracks the mean intensity of each volume (timepoint). Sudden increases and decreases in brain activity are reflected in this metric, potentially indicative of RF spikes and other acquisition artifacts affecting the entire volume. Final rows reflect percent volumes de-weighted due to motion (>0.5 mm volume-to-volume displacement) and global intensity (± 3 SD).

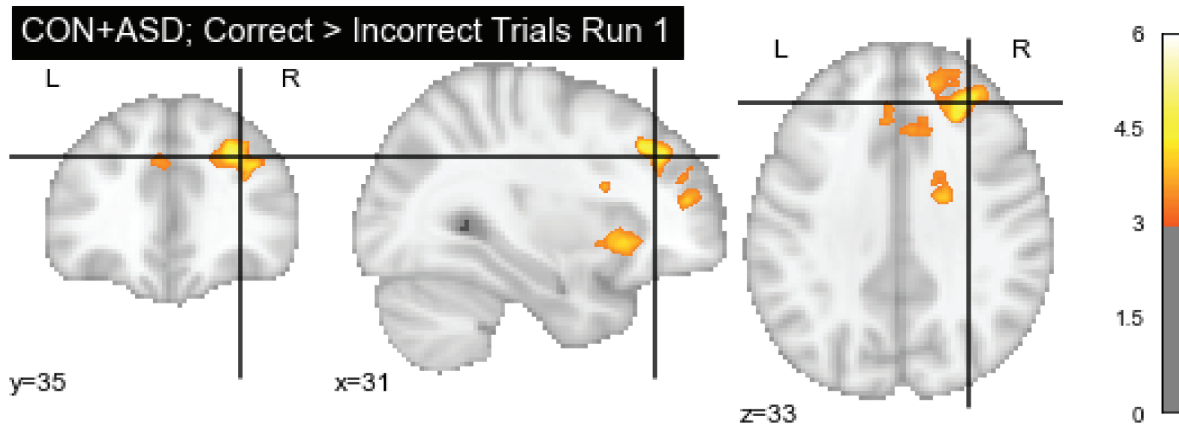
Support Vector Classification via Fast Regularized Ensemble of Models (Frem)

To further characterize spatial patterns of brain activation observed in run 1, we utilized an ROI-based forward prediction method as implemented in FReM to predict

behavioral responses in ‘never seen’ data in run 2. As the basis for this, all functionally derived clusters from run 1 that passed both height and FDR correction thresholds in distinguishing correct from incorrect judgments (which were observed only in the CON+ASD sample) were utilized for subsequent predictive analysis. We did not evaluate clusters describing the main effect for correct judgments only in the between-groups event-related analysis. The justification for probing only COR>INC within the full sample lies in the high potential for an unbalanced and therefore biased predictive design if evaluating a small number of events (i.e. only correct judgments, or roughly 20, on average) against all other events including rest trials (180 to 200 functional volumes for most participants). In this biased example, ‘good’ models would be those that predicted null for all outcomes (i.e. roughly 90% accuracy, in that example), as opposed to a comparatively more balanced design of correct and incorrect predictions that were not statistically different in their frequency in our sample.

Accordingly, we first examined clusters that distinguished between event types, specifically the ROIs that significantly differentiated COR from INC (as displayed in Table 5). We then applied the forward predictive models to the significant effects in shared mechanisms (CON+ASD) embodied by the four significant clusters (left and

A)



B)

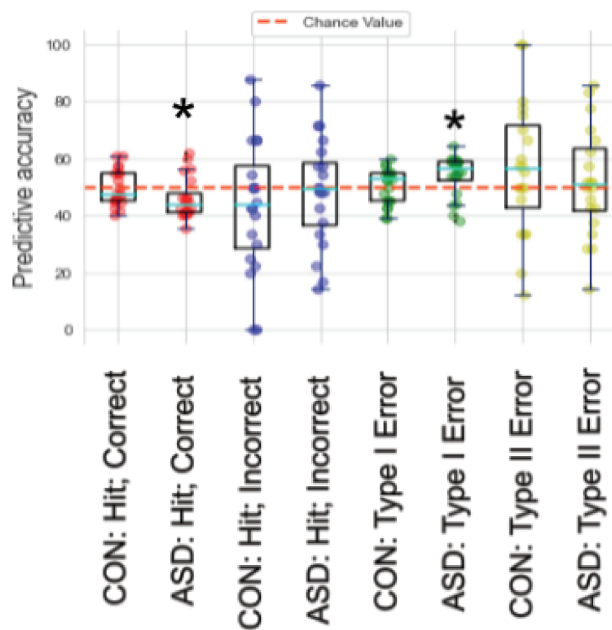


Figure 4. (A) Run 1: right dIPFC activation (all $ps < .001$; FDR corrected) shared between CON and ASD distinguishes between correct and incorrect decisions 2 s later. Note this cluster is also displayed in Figure 2, (panel B, green outline). Further note that only the dIPFC cluster targeted by the crosshair was used to generate the SVC-based predictive analysis below in panel B. (B) ROI-based prediction of behavior in run 2 using Support Vector Classification. Relative right dIPFC activation predicts false-positive decisions in ASD (neural data forecasts correct, but followed by incorrect emotion identification) but not controls, beyond chance rates. Asterisk denotes significant difference from chance (95% CI).

right insula, rACC and right dIPFC) that distinguished correct from incorrect responses (Figure 2, panel B, green outline). No significant results were observed for bilateral insula, again based on the finding that 95% confidence intervals for all event types included 0.50, or chance levels of prediction. However, the ACC ROI, as defined by COR>INC in run 1 (Figure 2, panel B, green outline; also Figure 3 panel A) yielded patterns of activation in run 2

that predicted correct facial emotion recognition beyond chance levels in CON ($M = 55.9\%$; 95% CI: 52.01–63.1), but not ASD ($M = 53.9\%$; 95% CI: 48.2–58.3). Figure 3, panel B displays the relative rates of accuracy as well as error rates for predicting correct and incorrect decisions, although it should be noted that although rates of accuracy in FReM prediction differed significantly from chance, they did not differ significantly between the two groups. We

then examined the fourth available ROI that distinguished correct from incorrect responses in both groups (CON +ASD; right dlPFC) and found that this ROI performed significantly worse than chance in predicting correct FER decisions among participants with ASD (Figure 4, panel B), and furthermore that this effect occurred in tandem with a higher than expected proportion of false-positive trials for ASD alone (i.e. neural model predicted correct decision, but behavioral response ultimately proved incorrect; $M = 53.9$; 95% CI: 52.4–60.34). By contrast, however, patterns of activity in this same cluster (right dlPFC) did not significantly predict false-positive errors among control participants ($M = 49.9$; 95% CI: 39.7–60.12). Thus, results of predictive modeling collectively suggest that the ACC and right dlPFC contributed distinct signals 2 s prior to both hits and errors for each of those outcomes.

Discussion

Accumulating evidence suggests that deficits in FER are common (Harms et al., 2010) and may mechanistically relate to social impairment by preventing accurate detection of social/emotional information conveyed through the face and subsequent deployment of emotionally appropriate responses. The current study sought to characterize the neural basis of FER in ASD by utilizing fMRI in conjunction with predictive statistical techniques to identify brain regions that forecast correct and incorrect choices about perceived facial emotions and the extent to which these regions were involved in correct decisions. Results of between-groups analysis indicated that a relatively constrained set of regions distinguished young men with ASD from typically developing peers 2 s prior to a correct decision about a facial emotion, including anterior cingulate, bilateral insula and right dorsolateral prefrontal cortex. However, no effects were observed when directly comparing regions that distinguished correct from incorrect judgments between groups. On the other hand, significant effects for correct > incorrect judgments were observed in the total sample (as well as main effects for both correct and incorrect choices), and results of SVC confirmed that the ACC was involved in subsequent correct choices for controls, but not ASD. Results from this machine learning approach furthermore revealed that activation patterns within the right dlPFC were predictive of Type I errors in ASD but not controls, suggesting that the right dlPFC may be the source of a false-positive signal regarding belief in a correct emotion identification (but followed by an incorrect judgment) among adolescent and young adults with ASD.

Machine learning approaches such as FReM provide useful information above and beyond traditional fMRI analysis by inverting the classical direction of inference and allowing conclusions to be drawn about a psychological state based on patterns of brain activation (Haynes, 2011). Our finding that the ACC was involved in correct FER judgments in controls is consistent with prior work suggesting that this region of the brain is involved in rapid processing of salient facial emotional information (Fan et al., 2011); however, its role in emotion recognition within ASD remains less clear. Uzefovsky et al. (2019) recently reported data from a sample of adolescents with ASD who completed the reading the mind in the eyes (RMET; a mental state judgment task based on interpretation of facial characteristics) task during fMRI. In this study, participants provided DNA samples for the purpose of genotyping seven single nucleotide polymorphisms (SNPs) related to the oxytocin receptor (OXTR). It was reported that high- and low-risk allele carriers were distinguishable on the basis of neural responses in the right supramarginal gyrus during the RMET, a cortical area that is notable for its moderate functional connectivity with the ACC (Du et al., 2020). Participants in the ASD group were significantly less accurate in their mental state judgments on the RMET as compared to a matched control group; however, once genotype was considered along with age and sex, this effect disappeared. Along similar lines (although not utilizing an ASD sample), Jack et al. (2012) found that activation in both the ACC and supramarginal gyrus during perception of social (versus random) shapes was related to methylation of OXTR, specifically that lower levels of methylation were associated with diminished activity in these regions. In contrast, however, heightened activation in the ACC was observed among adolescents and young adults with ASD during an emotion recognition task in a relatively early positron emission (PET) study conducted by Hall et al. (2003). Results suggested that a cross-modal (visual and auditory) emotion recognition task enhanced regional cerebral blood flow in the ACC among adults with ASD, a result which they speculate could have been due to the effect of crossmodal information as interfering with, rather than enhancing, facial emotion perception. This is potentially consistent with prior conceptualizations of ACC as a key location for the integration of affect (derived from anatomical connections with amygdala, ventral striatum and hippocampus), with areas important for cognition and executive function such as prefrontal cortex (Stevens et al., 2011). Etkin et al. (2011), in an integrated account of ACC subdivisions, proposed a role for the dorsal division of ACC (as observed in our task; e.g. Figure 3) in the appraisal of emotion,

particularly under conditions of conflict. Specifically, they propose that dorsal-caudal regions of the ACC are involved in the appraisal of emotion potentially by virtue of anatomical connections with dorsal and lateral prefrontal areas, which are important for top-down integration of context including current task requirements. In light of this account, results presented in the current study potentially bolster the argument that altered patterns of ACC activation may be related to systematic differences in conscious appraisal (exclusive of expression) of emotional responses and diminished integration of emotional context during situations with simultaneous cognitive demands.

Comparatively speaking, the right dlPFC did not contribute to success in facial emotion recognition but nonetheless revealed unique information about mechanisms of errors over decisions. Prior work has presupposed a role for dlPFC in valence attribution for emotional stimuli (Ferrari et al., 2017; Herrington et al., 2005; Nejati et al., 2021), as well as more general roles for goal-representation and working memory (Badre & Wagner, 2004; Kaller et al., 2011). We found that patterns of activation in this cortical region were exclusively related to errors in the ASD group, approximately 2 s prior to a button press indicating that the emotion was subjectively recognized. Cross validated results from SVC supported the utility of the right dlPFC in predicting errors, which builds upon experimental work in both ASD and non-ASD samples. For instance, in a sample of children (mean age 13.5 years) with ASD, Sokhadze et al. (2012) reported that repetitive transcranial magnetic stimulation (rTMS) over the dlPFC significantly reduced omission errors in a nonsocial (shape-matching oddball task), and further increased the amplitude of the error-related negativity (ERN) event-related potential (ERP). Similar effects have also been reported in non-ASD samples. Brennan et al. (2017) reported data from a randomized crossover placebo controlled trial among depressed adults, and found that transcranial direct current stimulation (tDCS) over dlPFC led to a significant improvement in FER as compared to placebo. A recent systematic review by Yamada et al. (2021) further supported this interpretation in psychiatric disorders and schizophrenia in particular, wherein anodal stimulation over the left dlPFC improved emotion recognition among schizophrenic patients (Rassovsky et al., 2015; Wölwer et al., 2014). Prior work using fMRI has also illustrated altered function in the dlPFC among adults with autism during conceptually related tasks including emotion regulation (Richey et al., 2015), perception of biological motion (Koldewyn et al., 2011), and a small number of studies have further revealed potential roles for the dlPFC

specifically in the context of face and emotion perception. Herrington et al. (2015) utilized a selective attention *n*-back task among children with ASD and typically developing controls during fMRI, in which images of faces and houses were superimposed. When attending to faces, children with ASD demonstrated increased activation in several prefrontal areas including dlPFC, and dlPFC activation was further correlated with increased response time for faces. Although accuracy in the *n*-back task did not differ between groups, heightened involvement of right dlPFC was interpreted in terms of task demands requiring greater selective attention among the ASD group in order to process the face percept.

In terms of overall accuracy of FER in the current study, we did not find evidence for systematic differences in the rates of correct versus incorrect judgments about faces between the ASD and control groups. At the behavioral level, however, the results of meta-analysis have previously supported the existence of a relatively large effect size in aggregate (-0.80) for behavioral markers of FER in ASD samples as compared to typically developing control participants (Uljarevic & Hamilton, 2013). Meta-analytic work has also supported the notion that emotion recognition is positively associated with everyday social functioning within ASD samples (Trevisan & Birmingham, 2016), and that the magnitude of these deficits increases with age and cannot be accounted for by intelligence (Lozier et al., 2014). FER targets, both behavioral and neural, may therefore represent a plausible focus for future intervention research in social-cognitive deficits among individuals with ASD. However, it should also be noted that improvements in social function were not found in a separate meta analysis demonstrating that intervention concepts that directly train FER abilities produce positive effects in actual emotion recognition abilities among children and adolescents with ASD (Zhang et al., 2021). Thus, the specific relationship between FER abilities and social functioning remains an ongoing question, particularly in the context of intervention research.

It should also be noted that FER deficits are not exclusive to autism. Indeed, it has become increasingly evident that such deficits in FER are not observed solely among children, adolescents and adults with ASD (Collin et al., 2013), nor do all individuals with ASD present with difficulties in recognizing facial emotion (Waddington et al., 2018). FER deficits have been observed among a number of neurological and neurodevelopmental disorders including individuals with intellectual disability (Zaja & Rojahn, 2008), schizophrenia (Johnston et al., 2005), parkinson's disease (Assogna et al., 2008) and among elderly adults (Sullivan &

Ruffman, 2004) as well as other psychiatric problems such as depression (Dalili et al., 2015). Thus, FER deficits may represent a transdiagnostic marker of socio-emotional disability that perhaps is particularly pronounced among individuals with ASD (Loth et al., 2018). In particular, Baron-Cohen et al. (1985) and Hobson (1986a; 1986b) were among the first to generally theorize that core deficits in ASD could, at least in part, be attributable to difficulties in encoding, recognizing and responding to emotional displays of an interaction partner. However, there is currently no presumption that all individuals with ASD necessarily demonstrate FER difficulties, and furthermore no assumption that such deficits exist across all types of facial expressions (happy, sad, disgust) or that these deficits are observed at the same level of intensity.

As with any study, results presented here should be evaluated in light of study limitations. A principal limitation that should be acknowledged here is that we do not have data available regarding individual ratings for certain characteristics of the stimuli (e.g. valence, arousal) used in this task, and so it cannot be affirmatively demonstrated whether decisions correlated with personal affective relevance of these images. Along similar lines, it is possible that gaze patterns differed between groups and because we do not have concurrent eye tracking data, it is possible that differential patterns of eye gaze could be driving these effects. Although it should further be noted that given the lack of accuracy differences between groups, it may be assumed that any gaze differences were negligible. Third, we utilized only dynamic images, whereas some have argued for a broad disadvantage for dynamic images in ASD (Sato et al., 2012). It should be noted however that this has been contradicted elsewhere (Enticott et al., 2014), and we further did not observe differences in the rates of accuracy between groups in our data, which likewise contradicts the notion that individuals with ASD are comparatively disadvantaged in recognition of emotion from dynamic images. Fourth, the sample contained only individuals self-identifying as male, and therefore results may not be generalizable to women with ASD. Future work should specifically focus on the extent to which the effects reported here are also characteristic of ASD as a whole, but more particularly whether they apply to women with ASD. Our decision to include only men was based upon both the preliminary nature of this work as well as the overall importance of controlling for as many relevant variables as possible, given the widely acknowledged heterogeneity inherent in this neurodevelopmental disorder. Fifth, previous FER studies have systematically examined the influence of

variables such as emotion type, amount of available time for decision-making and familiarity effects (Shanok et al., 2019). Although all stimuli in this study were presumed to be equally unfamiliar to all participants, we did not examine whether latencies were systematically different according to emotion type, mainly because we had relatively few samples of each specific emotional exemplar (six emotion types across 30 trials within each run resulted in 5 exemplars per run). Similarly, this related to another potential limitation, which is that we were unable to examine the rates of accuracy for specific emotion types in the event-related fMRI and follow up SVC analyses, due to relatively few examples of each event per participant. Next, the sample size was relatively small, which should be noted as a limitation. Lastly, although our sample was generally high functioning, limited information was available in our sample regarding the degree of social impairment and therefore we were not able to examine the extent to which neural results of FER may have related to functional disability. Future work should specifically focus on the extent to which neural markers of FER in this population are linked to clinical characteristics including social-emotional function. We also recommend future work aimed at identifying age-related effects of FER and underlying neural processes as revealed by our imaging task. Specifically, although we did not find evidence in our sample that age was related to either task-performance or imaging results, it is plausible that age may tangibly relate to FER expertise along a longer developmental timescale, which would provide further context for understanding the potential for intervention concepts to remediate basic processes reported here.

In conclusion, despite these limitations, results of the current study may provide unique insight into not only the neural mechanisms of FER broadly but also the utility of such markers to identify neural origins of systematic errors. Although we did not find evidence for differences in the rates of accuracy, nor for the involvement of subcortical areas in the prediction of correct or incorrect FER decisions, results are generally consistent with extant models of dysfunctional cortical-subcortical interactions in accurate judgments about facially displayed emotion. Specifically, our findings of altered cortical involvement may advance extant theories focused on the integration of affective dimensions with elaborative aspects of social cognition in limbic and cortical regions, respectively. Results presented here also represent preliminary verification of the neurobiological targets for behavioral measurement and potentially modification of FER. For example, the establishment of

replicable biomarkers is increasingly viewed as a prerequisite to development of neurotechnologies to remediate the clinical problem of FER impairment in particular (White et al., 2015). As such, the effects of both event-related fMRI as well as SVC reported here could be applicable to intervention research specifically within ASD as well as other clinical populations characterized by deficits in FER.

Disclosure Statement

All authors of this study report no conflict of interest, financial or otherwise.

Funding

This work was supported by the National Institutes of Health, National Institute of Mental Health (NIH/NIMH) under grant number MH100268.

References

- Abraham, A., Pedregosa, F., Eickenberg, M., Gervais, P., Mueller, A., Kossaifi, J., Gramfort, A., Thirion, B., & Varoquaux, G. (2014). Machine learning for neuroimaging with scikit-learn. *Frontiers in Neuroinformatics*, 8, 14. <https://doi.org/10.3389/fninf.2014.00014>
- Adolphs, R. (2002). Neural systems for recognizing emotion. *Current Opinion in Neurobiology*, 12(2), 169–177. [https://doi.org/10.1016/S0959-4388\(02\)00301-X](https://doi.org/10.1016/S0959-4388(02)00301-X)
- Anderson, M. C., Bunce, J. G., & Barbas, H. (2016). Prefrontal–hippocampal pathways underlying inhibitory control over memory. *Neurobiology of Learning and Memory*, 134, 145–161. <https://doi.org/10.1016/j.nlm.2015.11.008>
- Aoki, Y., Cortese, S., & Tansella, M. (2015). Neural bases of atypical emotional face processing in autism: A meta-analysis of fMRI studies. *The World Journal of Biological Psychiatry*, 16(5), 291–300. <https://doi.org/10.3109/15622975.2014.957719>
- Ashwin, C., Baron-Cohen, S., Wheelwright, S., O’Riordan, M., & Bullmore, E. T. (2007). Differential activation of the amygdala and the ‘social brain’ during fearful face-processing in Asperger Syndrome. *Neuropsychologia*, 45(1), 2–14. <https://doi.org/10.1016/j.neuropsychologia.2006.04.014>
- Assogna, F., Pontieri, F. E., Caltagirone, C., & Spalletta, G. (2008). The recognition of facial emotion expressions in Parkinson’s disease. *European Neuropsychopharmacology*, 18(11), 835–848. <https://doi.org/10.1016/j.euroneuro.2008.07.004>
- Avants, B. B., Tustison, N. J., Song, G., Cook, P. A., Klein, A., & Gee, J. C. (2011). A reproducible evaluation of ANTs similarity metric performance in brain image registration. *NeuroImage*, 54(3), 2033–2044. <https://doi.org/10.1016/j.neuroimage.2010.09.025>
- Badre, D., & Wagner, A. D. (2004). Selection, integration, and conflict monitoring: Assessing the nature and generality of prefrontal cognitive control mechanisms. *Neuron*, 41(3), 473–487. [https://doi.org/10.1016/S0896-6273\(03\)00851-1](https://doi.org/10.1016/S0896-6273(03)00851-1)
- Bar, M. (2003). A cortical mechanism for triggering top-down facilitation in visual object recognition. *Journal of Cognitive Neuroscience*, 15(4), 600–609. <https://doi.org/10.1162/089892903321662976>
- Bar, M. (2007). The proactive brain: Using analogies and associations to generate predictions. *Trends in Cognitive Sciences*, 11(7), 280–289. <https://doi.org/10.1016/j.tics.2007.05.005>
- Baron-Cohen, S., Jolliffe, T., Mortimore, C., & Robertson, M. (1997). Another advanced test of theory of mind: Evidence from very high functioning adults with autism or Asperger syndrome. *Journal of Child Psychology and Psychiatry, and Allied Disciplines*, 38(7), 813–822. <https://doi.org/10.1111/j.1469-7610.1997.tb01599.x>
- Baron-Cohen, S., Leslie, A. M., & Frith, U. (1985). Does the autistic child have a “theory of mind”? *Cognition*, 21(1), 37–46. [https://doi.org/10.1016/0010-0277\(85\)90022-8](https://doi.org/10.1016/0010-0277(85)90022-8)
- Barrera, M. E., & Maurer, D. (1981). The perception of facial expressions by the three-month-old. *Child Development*, 52(1), 203–206. <https://doi.org/10.2307/1129231>
- Barrett, L. F., Adolphs, R., Marsella, S., Martinez, A. M., & Pollak, S. D. (2019). Emotional expressions reconsidered: Challenges to inferring emotion from human facial movements. *Psychological Science in the Public Interest: A Journal of the American Psychological Society*, 20(1), 1–68. <https://doi.org/10.1177/1529100619832930>
- Batty, M., & Taylor, M. J. (2006). The development of emotional face processing during childhood. *Developmental Science*, 9(2), 207–220. <https://doi.org/10.1111/j.1467-7687.2006.00480.x>
- Black, M. H., Chen, N. T. M., Iyer, K. K., Lipp, O. V., Bölte, S., Falkmer, M., Tan, T., & Girdler, S. (2017). Mechanisms of facial emotion recognition in autism spectrum disorders: Insights from eye tracking and electroencephalography. *Neuroscience & Biobehavioral Reviews*, 80, 488–515. <https://doi.org/10.1016/j.neubiorev.2017.06.016>
- Boucher, O., Rouleau, I., Lassonde, M., Lepore, F., Bouthillier, A., & Nguyen, D. K. (2015). Social information processing following resection of the insular cortex. *Neuropsychologia*, 71, 1–10. <https://doi.org/10.1016/j.neuropsychologia.2015.03.008>
- Breiman, L. (1996). Bagging Predictors. *Machine Learning*, 24(2), 123–140. <https://doi.org/10.1007/BF00058655>
- Brennan, S., McLoughlin, D. M., O’Connell, R., Bogue, J., O’Connor, S., McHugh, C., & Glennon, M. (2017). Anodal transcranial direct current stimulation of the left dorsolateral prefrontal cortex enhances emotion recognition in depressed patients and controls. *Journal of Clinical and Experimental Neuropsychology*, 39(4), 384–395. <https://doi.org/10.1080/13803395.2016.1230595>
- Brown, T. A., & Barlow, D. H. (2014). *Anxiety and related disorders interview schedule for DSM-5 (ADIS-5L)*. Oxford University Press.
- Castelli, F. (2005). Understanding emotions from standardized facial expressions in autism and normal development. *Autism: The International Journal of Research and Practice*, 9(4), 428–449. <https://doi.org/10.1177/1362361305056082>
- Cohn, J. F., Zlochower, A. J., Lien, J., & Kanade, T. (1999). Automated face analysis by feature point tracking has high concurrent validity with manual FACS coding. *Psychophysiology*, 36(1), 35–43. <https://doi.org/10.1017/S0048577299971184>

- Collin, L., Bindra, J., Raju, M., Gillberg, C., & Minnis, H. (2013). Facial emotion recognition in child psychiatry: A systematic review. *Research in Developmental Disabilities, 34*(5), 1505–1520. <https://doi.org/10.1016/j.ridd.2013.01.008>
- Constantino, J. N., Davis, S. A., Todd, R. D., Schindler, M. K., Gross, M. M., Brophy, S. L., Metzger, L. M., Shoushtari, C. S., Splinter, R., & Reich, W. (2003). Validation of a brief quantitative measure of autistic traits: Comparison of the social responsiveness scale with the autism diagnostic interview-revised. *Journal of Autism and Developmental Disorders, 33*(4), 427–433. <https://doi.org/10.1023/A:1025014929212>
- Critchley, H. D., Daly, E. M., Bullmore, E. T., Williams, S. C., Van Amelsvoort, T., Robertson, D. M., Rowe, A., Phillips, M., McAlonan, G., Howlin, P., & Murphy, D. G. (2000). The functional neuroanatomy of social behaviour: Changes in cerebral blood flow when people with autistic disorder process facial expressions. *Brain: A Journal of Neurology, 123*(Pt 11), 2203–2212. <https://doi.org/10.1093/brain/123.11.2203>
- Dalili, M. N., Penton-Voak, I. S., Harmer, C. J., & Munafò, M. R. (2015). Meta-analysis of emotion recognition deficits in major depressive disorder. *Psychological Medicine, 45*(6), 1135–1144. <https://doi.org/10.1017/S0033291714002591>
- Deeley, Q., Daly, E. M., Surguladze, S., Page, L., Toal, F., Robertson, D., Curran, S., Giampietro, V., Seal, M., Brammer, M. J., Andrew, C., Murphy, K., Phillips, M. L., & Murphy, D. G. M. (2007). An event related functional magnetic resonance imaging study of facial emotion processing in Asperger syndrome. *Biological Psychiatry, 62*(3), 207–217. <https://doi.org/10.1016/j.biopsych.2006.09.037>
- Deichmann, R., Gottfried, J. A., Hutton, C., & Turner, R. (2003). Optimized EPI for fMRI studies of the orbitofrontal cortex. *NeuroImage, 19*(2), 430–441. [https://doi.org/10.1016/S1053-8119\(03\)00073-9](https://doi.org/10.1016/S1053-8119(03)00073-9)
- Domes, G., Kumbier, E., Heinrichs, M., & Herpertz, S. C. (2014). Oxytocin promotes facial emotion recognition and amygdala reactivity in adults with Asperger syndrome. *Neuropsychopharmacology, 39*(3), 698–706. <https://doi.org/10.1038/npp.2013.254>
- Du, J., Rolls, E. T., Cheng, W., Li, Y., Gong, W., Qiu, J., & Feng, J. (2020). Functional connectivity of the orbitofrontal cortex, anterior cingulate cortex, and inferior frontal gyrus in humans. *Cortex, 123*, 185–199. <https://doi.org/10.1016/j.cortex.2019.10.012>
- Ekman, P. (1970). Universal facial expressions of emotion. *California Mental Health Research Digest, 8*(4), 151–158.
- Ekman, P., & Friesen, W. V. (1978). *Manual for the facial action code*. Consulting Psychologist Press.
- Enticott, P. G., Kennedy, H. A., Johnston, P. J., Rinehart, N. J., Tonge, B. J., Taffe, J. R., & Fitzgerald, P. B. (2014). Emotion recognition of static and dynamic faces in autism spectrum disorder. *Cognition and Emotion, 28*(6), 1110–1118. <https://doi.org/10.1080/02699931.2013.867832>
- Etkin, A., Egner, T., & Kalisch, R. (2011). Emotional processing in anterior cingulate and medial prefrontal cortex. *Trends in Cognitive Sciences, 15*(2), 85–93. <https://doi.org/10.1016/j.tics.2010.11.004>
- Evers, K., Kerkhof, I., Steyaert, J., Noens, I., & Wagemans, J. (2014). No differences in emotion recognition strategies in children with autism spectrum disorder: Evidence from hybrid faces. *Autism Research and Treatment, 2014*, 345878. <https://doi.org/10.1155/2014/345878>
- Fan, J., Gu, X., Liu, X., Guise, K. G., Park, Y., Martin, L., de Marchena, A., Tang, C. Y., Minzenberg, M. J., & Hof, P. R. (2011). Involvement of the anterior cingulate and fronto-insular cortices in rapid processing of salient facial emotional information. *NeuroImage, 54*(3), 2539–2546. <https://doi.org/10.1016/j.neuroimage.2010.10.007>
- Ferrari, C., Gamond, L., Gallucci, M., Vecchi, T., & Cattaneo, Z. (2017). An exploratory TMS study on prefrontal lateralization in valence categorization of facial expressions. *Experimental Psychology, 64*(4), 282–289. <https://doi.org/10.1027/1618-3169/a000363>
- Fischl, B., Salat, D. H., van der Kouwe, A. J. W., Makris, N., Ségonne, F., Quinn, B. T., & Dale, A. M. (2004). Sequence-independent segmentation of magnetic resonance images. *NeuroImage, 23 Suppl 1*, S69–84. <https://doi.org/10.1016/j.neuroimage.2004.07.016>
- Fischl, B., van der Kouwe, A., Destrieux, C., Halgren, E., Ségonne, F., Salat, D. H., Busa, E., Seidman, L. J., Goldstein, J., Kennedy, D., Caviness, V., Makris, N., Rosen, B., & Dale, A. M. (2004). Automatically parcellating the human cerebral cortex. *Cerebral Cortex (New York, N. Y.: 1991), 14*(1), 11–22. <https://doi.org/10.1093/cercor/bhg087>
- Furl, N., Henson, R. N., Friston, K. J., & Calder, A. J. (2015). Network interactions explain sensitivity to dynamic faces in the superior temporal sulcus. *Cerebral Cortex (New York, N. Y.: 1991), 25*(9), 2876–2882. <https://doi.org/10.1093/cercor/bhu083>
- Gadde, S., Aucoin, N., Grethe, J. S., Keator, D. B., Marcus, D. S., & Pieper, S., & FBIRN, MBIRN, BIRN-CC. (2012). XCEDE: An extensible schema for biomedical data. *Neuroinformatics, 10*(1), 19–32. <https://doi.org/10.1007/s12021-011-9119-9>
- García-Villamizar, D., Rojahn, J., Zaja, R. H., & Jodra, M. (2010). Facial emotion processing and social adaptation in adults with and without autism spectrum disorder. *Research in Autism Spectrum Disorders, 4*(4), 755–762. <https://doi.org/10.1016/j.rasd.2010.01.016>
- Garman, H. D., Spaulding, C. J., Webb, S. J., Mikami, A. Y., Morris, J. P., & Lerner, M. D. (2016). Wanting it too much: an inverse relation between social motivation and facial emotion recognition in autism spectrum disorder. *Child Psychiatry & Human Development, 47*(6), 890–902. <https://doi.org/10.1007/s10578-015-0620-5>
- George, M. S., Ketter, T. A., Gill, D. S., Haxby, J. V., Ungerleider, L. G., Herscovitch, P., & Post, R. M. (1993). Brain regions involved in recognizing facial emotion or identity: An oxygen-15 PET study. *The Journal of Neuropsychiatry and Clinical Neurosciences, 5*(4), 384–394. <https://doi.org/10.1176/jnp.5.4.384>
- Goldman, A. I., & Sripada, C. S. (2005). Simulationist models of face-based emotion recognition. *Cognition, 94*(3), 193–213. <https://doi.org/10.1016/j.cognition.2004.01.005>
- Gorgolewski, K., Burns, C., Madison, C., Clark, D., Halchenko, Y., Waskom, M., & Ghosh, S. (2011). Nipype: A flexible, lightweight and extensible neuroimaging data processing framework in python. *Frontiers in Neuroinformatics, 5*, 13. <https://doi.org/10.3389/fninf.2011.00013>
- Greve, D. N., & Fischl, B. (2009). Accurate and robust brain image alignment using boundary-based registration. *NeuroImage, 48*(1), 63–72. <https://doi.org/10.1016/j.neuroimage.2009.06.060>

- Greve, D. N., Mueller, B. A., Liu, T., Turner, J. A., Voyvodic, J., Yetter, E., Diaz, M., McCarthy, G., Wallace, S., Roach, B. J., Ford, J. M., Mathalon, D. H., Calhoun, V. D., Wible, C. G., Potkin, S. G., & Glover, G. (2011). A novel method for quantifying scanner instability in fMRI. *Magnetic Resonance in Medicine*, 65(4), 1053–1061. <https://doi.org/10.1002/mrm.22691>
- Grossman, J. B., Klin, A., Carter, A. S., & Volkmar, F. R. (2000). Verbal bias in recognition of facial emotions in children with Asperger syndrome. *Journal of Child Psychology and Psychiatry, and Allied Disciplines*, 41(3), 369–379. <https://doi.org/10.1111/1469-7610.00621>
- Gu, X., Hof, P. R., Friston, K. J., & Fan, J. (2013). Anterior Insular cortex and emotional awareness. *The Journal of Comparative Neurology*, 521(15), 3371–3388. <https://doi.org/10.1002/cne.23368>
- Hadjikhani, N., Joseph, R. M., Snyder, J., & Tager-Flusberg, H. (2007). Abnormal activation of the social brain during face perception in autism. *Human Brain Mapping*, 28(5), 441–449. <https://doi.org/10.1002/hbm.20283>
- Hall, G. B. C., Szechtman, H., & Nahmias, C. (2003). Enhanced salience and emotion recognition in autism: A PET study. *American Journal of Psychiatry*, 160(8), 1439–1441. <https://doi.org/10.1176/appi.ajp.160.8.1439>
- Harms, M. B., Martin, A., & Wallace, G. L. (2010). Facial emotion recognition in autism spectrum disorders: A review of behavioral and neuroimaging studies. *Neuropsychology Review*, 20(3), 290–322. <https://doi.org/10.1007/s11065-010-9138-6>
- Haxby, J. V., Gobbini, M. I., Furey, M. L., Ishai, A., Schouten, J. L., & Pietrini, P. (2001). Distributed and overlapping representations of faces and objects in ventral temporal cortex. *Science*, 293(5539), 2425–2430. <https://doi.org/10.1126/science.1063736>
- Haynes, J. D. (2011). Multivariate decoding and brain reading: Introduction to the special issue. *NeuroImage*, 56(2), 385–386. <https://doi.org/10.1016/j.neuroimage.2011.03.057>
- Herrington, J. D., Mohanty, A., Koven, N. S., Fisher, J. E., Stewart, J. L., Banich, M. T., Webb, A. G., Miller, G. A., & Heller, W. (2005). Emotion-modulated performance and activity in left dorsolateral prefrontal cortex. *Emotion*, 5(2), 200–207. <https://doi.org/10.1037/1528-3542.5.2.200>
- Herrington, J. D., Riley, M. E., Grupe, D. W., & Schultz, R. T. (2015). Successful face recognition is associated with increased prefrontal cortex activation in autism spectrum disorder. *Journal of Autism and Developmental Disorders*, 45(4), 902–910. <https://doi.org/10.1007/s10803-014-2233-4>
- Herrington, J. D., Taylor, J. M., Grupe, D. W., Curby, K. M., & Schultz, R. T. (2011). Bidirectional communication between amygdala and fusiform gyrus during facial recognition. *NeuroImage*, 56(4), 2348–2355. <https://doi.org/10.1016/j.neuroimage.2011.03.072>
- Hess, U., Kafetsios, K., Mauersberger, H., Blaison, C., & Kessler, C.-L. (2016). Signal and noise in the perception of facial emotion expressions: From labs to life. *Personality and Social Psychology Bulletin*, 42(8), 1092–1110. <https://doi.org/10.1177/0146167216651851>
- Hobson, R. P. (1986a). The autistic child's appraisal of expressions of emotion. *Journal of Child Psychology and Psychiatry*, 27(3), 321–342. <https://doi.org/10.1111/j.1469-7610.1986.tb01836.x>
- Hobson, R. P. (1986b). The autistic child's appraisal of expressions of emotion: A further study. *Journal of Child Psychology and Psychiatry*, 27(5), 671–680.
- Hopkins, I. M., Gower, M. W., Perez, T. A., Smith, D. S., Amthor, F. R., Wimsatt, F. C., & Biasini, F. J. (2011). Avatar assistant: Improving social skills in students with an ASD through a computer-based intervention. *Journal of Autism and Developmental Disorders*, 41(11), 1543–1555. <https://doi.org/10.1007/s10803-011-1179-z>
- Hoyos-Idrobo, A., Varoquaux, G., Schwartz, Y., & Thirion, B. (2018). FReM – Scalable and stable decoding with fast regularized ensemble of models. *NeuroImage*, 180, 160–172. <https://doi.org/10.1016/j.neuroimage.2017.10.005>
- Humphreys, K., Hasson, U., Avidan, G., Minshew, N., & Behrmann, M. (2008). Cortical patterns of category-selective activation for faces, places and objects in adults with autism. *Autism Research: Official Journal of the International Society for Autism Research*, 1(1), 52–63. <https://doi.org/10.1002/aur.1>
- Jack, A., Connelly, J. J., & Morris, J. P. (2012). DNA methylation of the oxytocin receptor gene predicts neural response to ambiguous social stimuli. *Frontiers in Human Neuroscience*, 6. <https://doi.org/10.3389/fnhum.2012.00280>
- Johnston, P. J., Stojanov, W., Devir, H., & Schall, U. (2005). Functional MRI of facial emotion recognition deficits in schizophrenia and their electrophysiological correlates. *European Journal of Neuroscience*, 22(5), 1221–1232. <https://doi.org/10.1111/j.1460-9568.2005.04294.x>
- Jones, C. R. G., Pickles, A., Falcaro, M., Marsden, A. J. S., Happé, F., Scott, S. K., Sauter, D., Tregay, J., Phillips, R. J., Baird, G., Simonoff, E., & Charman, T. (2011). A multimodal approach to emotion recognition ability in autism spectrum disorders. *Journal of Child Psychology and Psychiatry, and Allied Disciplines*, 52(3), 275–285. <https://doi.org/10.1111/j.1469-7610.2010.02328.x>
- Kaller, C. P., Rahm, B., Spreer, J., Weiller, C., & Unterrainer, J. M. (2011). Dissociable contributions of left and right dorsolateral prefrontal cortex in planning. *Cerebral Cortex*, 21(2), 307–317. <https://doi.org/10.1093/cercor/bhq096>
- Kanade, T., Cohn, J. F., & Tian, Y. (2000). *Comprehensive Database for Facial Expression Analysis*. Proceedings of 4th IEEE International Conference on Automatic Face and Gesture Recognition, Washington DC, 28–30 March 2000, 46–53. <https://doi.org/10.1109/AFGR.2000.840611>
- Kanner, L. (1943). Autistic disturbances of affective contact. *Nervous Child*, 2, 217–250.
- Kawasaki, H., Tsuchiya, N., Kovach, C. K., Nourski, K. V., Oya, H., Howard, M. A., & Adolphs, R. (2012). Processing of facial emotion in the human fusiform gyrus. *Journal of Cognitive Neuroscience*, 24(6), 1358–1370. https://doi.org/10.1162/jocn_a_00175
- Kliemann, D., Dziobek, I., Hatri, A., Baudewig, J., & Heekeren, H. R. (2012). The role of the amygdala in atypical gaze on emotional faces in autism spectrum disorders. *Journal of Neuroscience*, 32(28), 9469–9476. <https://doi.org/10.1523/JNEUROSCI.5294-11.2012>

- Koldewyn, K., Whitney, D., & Rivera, S. M. (2011). Neural correlates of coherent and biological motion perception in autism: Motion perception in autism. *Developmental Science*, 14(5), 1075–1088. <https://doi.org/10.1111/j.1467-7687.2011.01058.x>
- Kveraga, K., Ghuman, A. S., & Bar, M. (2007). Top-down predictions in the cognitive brain. *Brain and Cognition*, 65(2), 145–168. <https://doi.org/10.1016/j.bandc.2007.06.007>
- LaConte, S. M. (2011). Decoding fMRI brain states in real-time. *NeuroImage*, 56(2), 440–454. <https://doi.org/10.1016/j.neuroimage.2010.06.052>
- LaConte, S., Strother, S., Cherkassky, V., Anderson, J., & Hu, X. (2005). Support vector machines for temporal classification of block design fMRI data. *NeuroImage*, 26(2), 317–329. <https://doi.org/10.1016/j.neuroimage.2005.01.048>
- Lacroix, A., Guidetti, M., Rogé, B., & Reilly, J. (2009). Recognition of emotional and nonemotional facial expressions: A comparison between Williams syndrome and autism. *Research in Developmental Disabilities*, 30(5), 976–985. <https://doi.org/10.1016/j.ridd.2009.02.002>
- Lane, R., Fink, G., Chau, P. M., & Dolan, R. (1997). Neural activation during selective attention to subjective emotional responses. *Neuroreport*, 8(18), 3969–3972. <https://doi.org/10.1097/00001756-199712220-00024>
- Lenti, C., Lenti-Boero, D., & Giacobbe, A. (1999). Decoding of emotional expressions in children and adolescents. *Perceptual and Motor Skills*, 89(3 Pt 1), 808–814. <https://doi.org/10.2466/pms.1999.89.3.808>
- Leppänen, J. M., & Nelson, C. A. (2009). Tuning the developing brain to social signals of emotions. *Nature Reviews Neuroscience*, 10(1), 37–47. <https://doi.org/10.1038/nrn2554>
- Lindquist, K. A., Wager, T. D., Kober, H., Bliss-Moreau, E., & Barrett, L. F. (2012). The brain basis of emotion: A meta-analytic review. *Behavioral and Brain Sciences*, 35(3), 121–143. <https://doi.org/10.1017/S0140525X11000446>
- Lord, C., Rutter, M., DiLavore, P. C., Risi, S., Gotham, K., & Bishop, S. (2012). *Autism Diagnostic Observation Schedule* (2nd ed.). Western Psychological Services.
- Loth, E., Garrido, L., Ahmad, J., Watson, E., Duff, A., & Duchaine, B. (2018). Facial expression recognition as a candidate marker for autism spectrum disorder: How frequent and severe are deficits? *Molecular Autism*, 9(1), 7. <https://doi.org/10.1186/s13229-018-0187-7>
- Lozier, L. M., Vanmeter, J. W., & Marsh, A. A. (2014). Impairments in facial affect recognition associated with autism spectrum disorders: A meta-analysis. *Development and Psychopathology*, 26(4pt1), 933–945. <https://doi.org/10.1017/S0954579414000479>
- Lucey, P., Cohn, J. F., Kanade, T., Saragih, J., Ambadar, Z., & Matthews, I. (2010). The Extended Cohn-Kanade Dataset (CK+): A complete dataset for action unit and emotion-specified expression. *2010 IEEE Computer Society Conference on Computer Vision and Pattern Recognition - Workshops*, 94–101. <https://doi.org/10.1109/CVPRW.2010.5543262>
- Macdonald, H., Rutter, M., Howlin, P., Rios, P., Conteur, A. L., Evered, C., & Folstein, S. (1989). Recognition and expression of emotional cues by autistic and normal adults. *Journal of Child Psychology and Psychiatry*, 30(6), 865–877. <https://doi.org/10.1111/j.1469-7610.1989.tb00288.x>
- Matykievicz, P., & Pestian, J. (2012). Effect of small sample size on text categorization with support vector machines. *Proceedings of the 2012 Workshop on Biomedical Natural Language Processing*, 193–201.
- Medford, N., & Critchley, H. D. (2010). Conjoint activity of anterior insular and anterior cingulate cortex: Awareness and response. *Brain Structure & Function*, 214(5–6), 535–549. <https://doi.org/10.1007/s00429-010-0265-x>
- Mier, D., Lis, S., Neuthe, K., Sauer, C., Esslinger, C., Gallhofer, B., & Kirsch, P. (2010). The involvement of emotion recognition in affective theory of mind. *Psychophysiology*, 47(6), 1028–1039. <https://doi.org/10.1111/j.1469-8986.2010.01031.x>
- Nejati, V., Majdi, R., Salehinejad, M. A., & Nitsche, M. A. (2021). The role of dorsolateral and ventromedial prefrontal cortex in the processing of emotional dimensions. *Scientific Reports*, 11(1), 1971. <https://doi.org/10.1038/s41598-021-81454-7>
- Nuske, H. J., Vivanti, G., & Dissanayake, C. (2013). Are emotion impairments unique to, universal, or specific in autism spectrum disorder? A comprehensive review. *Cognition & Emotion*, 27(6), 1042–1061. <https://doi.org/10.1080/02699931.2012.762900>
- Ogai, M., Matsumoto, H., Suzuki, K., Ozawa, F., Fukuda, R., Uchiyama, I., Suckling, J., Isoda, H., Mori, N., & Takei, N. (2003). fMRI study of recognition of facial expressions in high-functioning autistic patients. *Neuroreport*, 14(4), 559–563. <https://doi.org/10.1097/00001756-200303240-00006>
- Pelphrey, K. A., Morris, J. P., & McCarthy, G. (2005). Neural basis of eye gaze processing deficits in autism. *Brain: A Journal of Neurology*, 128(Pt 5), 1038–1048. <https://doi.org/10.1093/brain/awh404>
- Pourtois, G., Schettino, A., & Vuilleumier, P. (2013). Brain mechanisms for emotional influences on perception and attention: What is magic and what is not. *Biological Psychology*, 92(3), 492–512. <https://doi.org/10.1016/j.biopsycho.2012.02.007>
- Rassovsky, Y., Dunn, W., Wynn, J., Wu, A. D., Iacoboni, M., Helleman, G., & Green, M. F. (2015). The effect of transcranial direct current stimulation on social cognition in schizophrenia: A preliminary study. *Schizophrenia Research*, 165(2–3), 171–174. <https://doi.org/10.1016/j.schres.2015.04.016>
- Richey, J. A., Damiano, C. R., Sabatino, A., Rittenberg, A., Petty, C., Bizzell, J., Voyvodic, J., Heller, A. S., Coffman, M. C., Smoski, M., Davidson, R. J., & Dichter, G. S. (2015). Neural mechanisms of emotion regulation in autism spectrum disorder. *Journal of Autism and Developmental Disorders*, 45(11), 3409–3423. <https://doi.org/10.1007/s10803-015-2359-z>
- Said, C. P., Moore, C. D., Engell, A. D., Todorov, A., & Haxby, J. V. (2010). Distributed representations of dynamic facial expressions in the superior temporal sulcus. *Journal of Vision*, 10(5), 11. <https://doi.org/10.1167/10.5.11>
- Sato, W., Toichi, M., Uono, S., & Kochiyama, T. (2012). Impaired social brain network for processing dynamic facial expressions in autism spectrum disorders. *BMC Neuroscience*, 13(1), 99. <https://doi.org/10.1186/1471-2202-13-99>
- Scherf, K. S., Luna, B., Minshew, N., & Behrmann, M. (2010). Location, location, location: alterations in the functional topography of face- but not object- or place-related cortex in adolescents with autism. *Frontiers in Human Neuroscience*, 4, 26. <https://doi.org/10.3389/fnhum.2010.00026>

- Schultz, J., & Pilz, K. S. (2009). Natural facial motion enhances cortical responses to faces. *Experimental Brain Research*, 194(3), 465–475. <https://doi.org/10.1007/s00221-009-1721-9>
- Shalev-Shwartz, S., Shamir, O., Srebro, N., & Sridharan, K. (2010). Learnability, stability and uniform convergence. *The Journal of Machine Learning Research*, 11, 2635–2670.
- Shanok, N. A., Jones, N. A., & Lucas, N. N. (2019). The nature of facial emotion recognition impairments in children on the autism spectrum. *Child Psychiatry & Human Development*, 50(4), 661–667. <https://doi.org/10.1007/s10578-019-00870-z>
- Shanton, K., & Goldman, A. (2010). Simulation theory. *Wiley Interdisciplinary Reviews. Cognitive Science*, 1(4), 527–538. <https://doi.org/10.1002/wcs.33>
- Smith, S. M. (2002). Fast robust automated brain extraction. *Human Brain Mapping*, 17(3), 143–155. <https://doi.org/10.1002/hbm.10062>
- Sokhadze, E. M., Baruth, J. M., Sears, L., Sokhadze, G. E., El-Baz, A. S., & Casanova, M. F. (2012). Prefrontal neuromodulation using rTMS improves error monitoring and correction function in autism. *Applied Psychophysiology and Biofeedback*, 37(2), 91–102. <https://doi.org/10.1007/s10484-012-9182-5>
- Spezio, M. L., Adolphs, R., Hurley, R. S. E., & Piven, J. (2007). Abnormal use of facial information in high-functioning autism. *Journal of Autism and Developmental Disorders*, 37(5), 929–939. <https://doi.org/10.1007/s10803-006-0232-9>
- Stevens, F. L., Hurley, R. A., Taber, K. H., Hurley, R. A., Hayman, L. A., & Taber, K. H. (2011). Anterior cingulate cortex: unique role in cognition and emotion. *The Journal of Neuropsychiatry and Clinical Neurosciences*, 23(2), 121–125. <https://doi.org/10.1176/jnp.23.2.jnp121>
- Styliadis, C., Leung, R., Özcan, S., Moulton, E. A., Pang, E., Taylor, M. J., & Papadelis, C. (2021). Atypical spatio-temporal activation of cerebellar lobules during emotional face processing in adolescents with autism. *Human Brain Mapping*, 42(7), 2099–2114. <https://doi.org/10.1002/hbm.25349>
- Sugranyes, G., Kyriakopoulos, M., Corrigall, R., Taylor, E., Frangou, S., & Baune, B. T. (2011). Autism spectrum disorders and schizophrenia: Meta-analysis of the neural correlates of social cognition. *PLoS ONE*, 6(10), e25322. <https://doi.org/10.1371/journal.pone.0025322>
- Sullivan, S., & Ruffman, T. (2004). Emotion recognition deficits in the elderly. *International Journal of Neuroscience*, 114(3), 403–432. <https://doi.org/10.1080/00207450490270901>
- Trevisan, D. A., & Birmingham, E. (2016). Are emotion recognition abilities related to everyday social functioning in ASD? A meta-analysis. *Research in Autism Spectrum Disorders*, 32, 24–42. <https://doi.org/10.1016/j.rasd.2016.08.004>
- Turner, J. H., & Stets, J. E. (2006). Sociological Theories of Human Emotions. *Annual Review of Sociology*, 32(1), 25–52. <https://doi.org/10.1146/annurev.soc.32.061604.123130>
- Uljarevic, M., & Hamilton, A. (2013). Recognition of emotions in autism: A formal meta-analysis. *Journal of Autism and Developmental Disorders*, 43(7), 1517–1526. <https://doi.org/10.1007/s10803-012-1695-5>
- Uzefovsky, F., Bethlehem, R. A. I., Shamay-Tsoory, S., Ruigrok, A., Holt, R., Spencer, M., Chura, L., Warrier, V., Chakrabarti, B., Bullmore, E., Suckling, J., Floris, D., & Baron-Cohen, S. (2019). The oxytocin receptor gene predicts brain activity during an emotion recognition task in autism. *Molecular Autism*, 10(1), 12. <https://doi.org/10.1186/s13229-019-0258-4>
- Vuilleumier, P., & Pourtois, G. (2007). Distributed and interactive brain mechanisms during emotion face perception: Evidence from functional neuroimaging. *Neuropsychologia*, 45(1), 174–194. <https://doi.org/10.1016/j.neuropsychologia.2006.06.003>
- Waddington, F., Hartman, C., de Bruijn, Y., Lappenschaar, M., Oerlemans, A., Buitelaar, J., Franke, B., & Rommelse, N. (2018). An emotion recognition subtyping approach to studying the heterogeneity and comorbidity of autism spectrum disorders and attention-deficit/hyperactivity disorder. *Journal of Neurodevelopmental Disorders*, 10(1), 31. <https://doi.org/10.1186/s11689-018-9249-6>
- Wallace, G. L., Case, L. K., Harms, M. B., Silvers, J. A., Kenworthy, L., & Martin, A. (2011). Diminished sensitivity to sad facial expressions in high functioning autism spectrum disorders is associated with symptomatology and adaptive functioning. *Journal of Autism and Developmental Disorders*, 41(11), 1475–1486. <https://doi.org/10.1007/s10803-010-1170-0>
- Wechsler, D. (2011). *Wechsler abbreviated scale of intelligence—Second Edition (WASI-II)*. NCS Pearson.
- White, S. W., Richey, J. A., Gracanin, D., Bell, M. A., LaConte, S., Coffman, M., Trubanova, A., & Kim, I. (2015). The promise of neurotechnology in clinical translational science. *Clinical Psychological Science*, 3(5), 797–815. <https://doi.org/10.1177/2167702614549801>
- Wilson-Mendenhall, C. D., Barrett, L. F., Simmons, W. K., & Barsalou, L. W. (2011). Grounding emotion in situated conceptualization. *Neuropsychologia*, 49(5), 1105–1127. <https://doi.org/10.1016/j.neuropsychologia.2010.12.032>
- Wölwer, W., Lowe, A., Brinkmeyer, J., Streit, M., Habakuck, M., Agelink, M. W., Mobascher, A., Gaebel, W., & Cordes, J. (2014). Repetitive transcranial magnetic stimulation (rTMS) improves facial affect recognition in schizophrenia. *Brain Stimulation*, 7(4), 559–563. <https://doi.org/10.1016/j.brs.2014.04.011>
- Wood, A., Rychlowska, M., Korb, S., & Niedenthal, P. (2016). Fashioning the Face: Sensorimotor Simulation Contributes to Facial Expression Recognition. *Trends in Cognitive Sciences*, 20(3), 227–240. <https://doi.org/10.1016/j.tics.2015.12.010>
- Yamada, Y., Inagawa, T., Hirabayashi, N., & Sumiyoshi, T. (2021). Emotion recognition deficits in psychiatric disorders as a target of non-invasive neuromodulation: A systematic review. *Clinical EEG and Neuroscience*, 1–7. <https://doi.org/10.1177/1550059421991688>
- Zaja, R. H., & Rojahn, J. (2008). Facial emotion recognition in intellectual disabilities. *Current Opinion in Psychiatry*, 21(5), 441–444. <https://doi.org/10.1097/YCO.0b013e328305e5fd>
- Zhang, Q., Wu, R., Zhu, S., Le, J., Chen, Y., Lan, C., Yao, S., Zhao, W., & Kendrick, K. M. (2021). Facial emotion training as an intervention in autism spectrum disorder: A meta-analysis of randomized controlled trials. *Autism Research*, 14(10), aur.2565. <https://doi.org/10.1002/aur.2565>